KINETICS AND MECHANISMS OF INTERACTIONS OF NITROGEN AND CARBON MONOXIDE WITH LIQUID NIOBIUM

By

HYUN GYOON PARK

A DISSERTATION PRESENTED TO THE GRADUATE SCHOOL
OF THE UNIVERSITY OF FLORIDA IN PARTIAL FULFILLMENT
OF THE REQUIREMENTS FOR THE DEGREE OF
DOCTOR OF PHILOSOPHY

UNIVERSITY OF FLORIDA

1990

TO MY PARENTS

ACKNOWLEDGMENTS

The author wishes to express his deepest gratitude and appreciation to his supervisory committee chairman, Dr. Reza Abbaschian, for his guidance, support, and patience throughout this research. He also would like to acknowledge and thank the members of his graduate committee, Dr. Robert T. DeHoff, Dr. Paul H. Holloway, Dr. Brij M. Moudgil, and Dr. Dinesh O. Shah.

Special thanks goes to the NASA Vanderbilt Center for the Space Processing of Engineering Materials for its funding of this work. Special thanks are also extended to Dr. P. Kumar of Cabot Corporation for his useful and illuminating discussions during the course of this work and to Cabot Corporation for supplying the Nb used in this work and also the prompt composition analysis of the interstitial content. The author is thankful to his coworkers in materials processing group, especially to Atul B. Gokhale, with whom he had many fruitful discussions on various aspects of this research.

The author wishes to express a deep heartfelt appreciation to his mother, brothers, and sisters for their financial support and encouragement.

Finally, an indescribable degree of appreciation goes to the author's wife, Myung Suk, and sons, Hwan Seong and Joon Seong, for their continuous support, patience, and encouragement throughout his stay in the U.S.A.

TABLE OF CONTENTS

page

ACKNOWLEDGMENTS iii

LIST OF TABLES vi

LIST OF FIGURES vii

ABSTRACT xi

INTRODUCTION 1

REVIEW OF LITERATURE 7

- Thermodynamics of Solution 8
- Solubility of Gases in Metals 13
- Deoxidation by Reduction Processes or by Evaporation of Suboxides 21
  - Reduction by Carbon or Hydrogen 21
  - Deoxidation by Evaporation of Suboxides 23
- Phase Diagrams and Thermodynamic Data 26
  - Nb - N System 26
  - Nb - O System 30
  - Nb - C system 36
- Reaction Rate 41
- Rate Controlling Step 42
- Effect of Temperature on Reaction Rate 45
- Energetics of Reaction Path 48
- Kinetic Models on High Temperature Gas/Metal Reactions 51
  - Mass Transfer in the Gas Phase 53
  - Transport in Liquid Phase 57
  - Interface Chemical Reaction 60
- Reactions under Dissociation and Formation of Carbon Monoxide 66

EXPERIMENTAL 73

- Electromagnetic Levitation Technique 73
- Materials 75
- Apparatus 78
- Procedures 80
- Quadrupole Mass Spectrometry 83

EXPERIMENTAL RESULTS 84

- Nitrogen 84
  - Effect of Gas Flow Rate on Nitrogen Absorption 84
  - Effect of Temperature on Nitrogen Absorption 86
  - Effect of Nitrogen Partial Pressure on Nitrogen Absorption 86
  - Nitrogen Desorption 91
- Carbon Monoxide 91
  - Effect of CO Partial Pressure on C and O Absorption 94
  - Effect of Temperature on C and O Absorption 94
  - Effect of Gas Flow Rate on C and O Absorption 99
  - Gas Phases Analysis by Quadrupole Mass Spectrometer 103
  - C and O Desorption 105

DISCUSSION 112

- Nitrogen 112
  - Solubility of Nitrogen 112
  - Reaction Sequence 116
  - Characteristics of Each Elementary Step 119
  - The Order of Reaction and Rate Controlling Step 122
  - Reaction Rates of Nitrogen Absorption and Desorption 136
- Carbon Monoxide 138
  - Solubilities of C and O under CO Atmosphere 138
  - Reaction Sequence in CO Liquid Nb Interaction 140
  - The Order of Reaction and Rate Controlling Step in CO Absorption 149
  - Temperature Dependence of Absorption Rate Equation 159
  - The Order of Reaction and Rate Equation for CO Desorption 163

CONCLUSION 168

REFERENCES 171

BIOGRAPHICAL SKETCH 176

LIST OF TABLES

1 Property changes of Nb due to 1 at.% dissolved H, N, O, and C at ambient temperature 3

2 Typical purity of niobium before and after electron beam melting 5

3 Thermodynamic data and evaporation ratios relating to the deoxidation of refractory metals in solid state 25

4. Thermodynamic data associated with Nb–N system 28

5 Thermodynamic data associated with Nb–O system 34

6. Thermodynamic data associated with Nb–C system 39

7 Chemical analysis of Nb 76

8 Composition analysis of gases 77

9 Summary of the characteristics of each elementary step as a rate controlling step 123

10 Apparent activation energies on CO–liquid niobium reaction 162

LIST OF FIGURES

1.1 Effect of dissolved gases on the mechanical and electrical properties of recrystallized niobium 2

2.1 Examples of the relationship between vapor pressure and concentration in a binary system A-B with a positive deviation from Raoult's Law 12

2.2 Solubilities of gases in liquid iron at 1600 °C, in liquid nickel at 1450 °C and liquid chromium at 1745 °C 15

2.3 Temperature dependence of the oxygen pressure of copper, iron and nickel containing 100 ppm oxygen and of the vapor pressure of the pure metals 17

2.4 Solubilities of nitrogen in solid Nb, Ta, Cr, Mo, W and Re 18

2.5 Oxygen pressure as a function of the oxygen content of pure iron pure nickel and several iron-nickel alloys at 1600 °C 20

2.6 Equilibrium vapor pressure over the Nb-O and Nb-C-O solid solutions at 2273 K 22

2.7 Nb - N phase diagram 27

2.8 Pressure - concentration isotherm in Nb - N system 29

2.9 Nb - N system, log P - log C_N diagram at the melting point of Nb 31

2.10 Nb - O phase diagram 32

2.11 Steady state during annealing of Nb in O_2 atmosphere 35

2.12 Evaporation rates of Nb in O_2 37

2.13 Nb - C phase diagram 38

2.14 Equilibrium pressure of CO over Nb-C-O solid solution with the ratio of C to O equal to unity 40

2.15 Rate of a reaction(A) consisting of two partial reactions (B and

C) which are both rate determining 47

2.16 Energy diagrams for reversible absorption and desorption of diatomic gases A_2 49

2.17 Concentration and partial pressure profile for different types of rate control in degassing process 52

2.18 Reaction coefficients for the absorption of oxygen or nitrogen in the system V-O, Nb-O, or Ta-O, or Nb-N as a function of the reciprocal absolute temperature 67

2.19 Correlation of the carbon and oxygen levels in niobium before and after the vacuum degassing in solid state 69

2.20 Correlation of the carbon and oxygen levels in niobium before and after melting in the electron beam furnace for 600 seconds 70

2.21 Reaction scheme for the decarburization of Vb metals in flowing oxygen 72

3.1 Schematic diagram of levitation coil 74

3.2 Schematic diagram of experimental set up 79

4.1 Nitrogen absorption behavior of liquid Nb as a function of gas flow rate 85

4.2 Effect of temperature on nitrogen absorption in liquid Nb (a) P_{N_2} = 0.25 atm (b) P_{N_2} = 0.15 atm (c) P_{N_2} = 0.05 atm 87

4.3 Typical temperature profile during nitrogen absorption 90

4.4 Effect of nitrogen partial pressure on nitrogen absorption in liquid Nb 92

4.5 Typical nitrogen desorption behavior in liquid Nb 93

4.6 Effect of CO partial pressure on carbon absorption in liquid Nb 95

4.7 Effect of CO partial pressure on oxygen absorption in liquid Nb 96

4.8 Effect of temperature on carbon absorption from CO in liquid Nb 97

4.9 Effect of temperature on oxygen absorption from CO in liquid Nb 98

4.10 Interrelationship between oxygen and carbon concentrations during CO absorption 100

4.11 Carbon absorption behavior of Nb from CO gas as a function of gas flow rate 101

4.12 Oxygen absorption behavior of Nb from CO gas as a function of gas flow rate 102

4.13 Changes of partial pressures of CO and CO_2 of outlet gas during C and O absorption from CO gas 104

4.14 Effect of partial pressure of CO on carbon desorption in liquid Nb 106

4.15 Effect of partial pressure of CO on oxygen desorption in liquid Nb 107

4.16 Effect of temperature on carbon desorption in liquid Nb under pure Ar
(a) raw data (b) normalized concentration against initial concentration 108

4.17 Effect of temperature on oxygen desorption in liquid Nb under pure Ar
(a) raw data (b) normalized concentration against initial concentration 109

4.18 Interrelationship between the desorbed amounts of oxygen and carbon in atomic % during CO desorption 111

5.1 Plot of equilibrium concentration as a function of $P_{N_2}^{1/2}$ at various temperatures 114

5.2 Arrhenius type plot of log k, Sievert constant, versus 1/T 115

5.3 Reaction mechanism of nitrogen absorption/desorption in liquid Nb 117

5.4 Effect of gas flow rate on the second order rate constant for nitrogen absorption in liquid Nb 125

5.5 Kinetics of nitrogen absorption into liquid Nb under various partial pressure of nitrogen correlated with first order rate equation 128

5.6 Kinetics of nitrogen absorption into liquid Nb under various partial pressure of nitrogen correlated with second order rate equation 131

5.7 Kinetics of nitrogen desorption from liquid Nb under various partial pressures of nitrogen correlated with first order rate equation 134

5.8 Kinetics of nitrogen desorption from liquid Nb under various partial pressures of nitrogen correlated with second order rate equation 135

5.9 Effect of temperature on second order rate constant, k, of nitrogen absorption 137

5.10 Relationship between equilibrium carbon and oxygen concentrations and partial pressure of CO 139

5.11 Relationship between Ln(C_{Ce}·C_{Oe}/P_{co}) and 1/T 141

5.12 Reaction paths during CO absorption and desorption 145

5.13 Mechanism of carbon and oxygen dissolution in liquid Nb from CO gas 146

5.14 Carbon absorption kinetics correlated with first order rate equation 154

5.15 Oxygen absorption kinetics correlated with first order rate equation 155

5.16 Carbon absorption kinetics correlated with second order rate equation 157

5.17 Oxygen absorption kinetics correlated with second order rate equation 158

5.18 Second order plot of carbon absorption data at various temperatures 160

5.19 Arrhenius type plot of second order rate constants on carbon absorption in CO atmosphere 161

5.20 First order plot of oxygen desorption kinetics in atmospheres with various partial pressures of CO 164

5.21 Second order plot of oxygen desorption kinetics in atmospheres with various partial pressures of CO 165

5.22 Second order plot of oxygen desorption data in pure Ar atmosphere obtained at various temperatures 166

5.23 Plot of Ln k, second order rate constant of oxygen desorption in pure Ar, versus 1/T 167

Abstract of Dissertation Presented to the Graduate School
of the University of Florida in Partial Fulfillment of the
Requirements For the Degree of Doctor of Philosophy

KINETICS AND MECHANISMS OF INTERACTIONS OF NITROGEN AND CARBON MONOXIDE WITH LIQUID NIOBIUM

By

HYUN GYOON PARK

December 1990

Chairman Dr Reza Abbaschian
Major Department Materials Science and Engineering

The kinetics and mechanisms of interactions of nitrogen and carbon monoxide with liquid niobium were investigated in the temperature range of 2700 to 3000 K in samples levitated in N_2/Ar and CO/Ar streams

The nitrogen solution reaction in liquid niobium was found to be exothermic with the standard enthalpy and entropy of solution of -236.4 ± 23.3 kJ/mol and 65.3 ± 8.3 J/K•mol, respectively. Accordingly the nitrogen solubility (C_N, in wt%) is expressed as

$$\log C_N = \frac{12330}{T} - 3.41 + 1/2 \log P_{N_2}$$

where T is the temperature in K, and P_{N_2} is the nitrogen partial pressure in atm.

The nitrogen absorption and desorption processes were found to be second order with respect to nitrogen concentration, indicating that the rate controlling step

is either the adsorption of nitrogen molecules on the liquid surface or dissociation of adsorbed nitrogen molecules into adsorbed atoms. The rate equations for nitrogen absorption and desorption are given by

$$\left(\frac{dC_N}{dt}\right)_{abs} = 2.290\cdot10^3 \exp\left(\frac{39200}{T}\right)\frac{A}{V}(C_{Ns}^2 - C_N^2)$$

and

$$\left(\frac{dC_N}{dt}\right)_{des} = 1.680\cdot10^7 \exp\left(\frac{67500}{T}\right)\frac{A}{V}(C_{Ne}^2 \quad C_N^2)$$

where C_N is the nitrogen concentration in wt%. A is the surface area in Cm^2, V is the volume in Cm^3

The carbon and oxygen dissolution in liquid niobium from CO gas is also an exothermic process and the solubilities of carbon and oxygen (C_{Ce}, C_{Oe} in at%) are related to the temperature and the partial pressure of CO (P_{co} in atm) as

$$\ln C_{Ce} + \ln C_{Oe} \quad \ln P_{co} = 2.32\cdot10^4/T \quad 2.35$$

The reaction CO -> [C] + [O] along with the evaporation of niobium oxide takes place during C and O dissolution, whereas C and O desorption occurs via CO evolution only, especially when excess carbon exists in the liquid. Absorption /desorption of carbon and oxygen in liquid niobium are second order processes with the first order dependence on C and O concentrations (C_C, C_O in at%) respectively, implying that the overall reaction rate is controlled by the substep of dissociation of adsorbed CO molecules(or recombination of C and O in the case of desorption) The rate equations for C and O dissolution and desorption are found to be

$$(dC_C/dt)_{abs} = (1/0.76)(dC_O/dt)_{abs} = 12.1(A/V)\exp(26700/T)(C_{Ce}C_{Oe} - C_CC_O)$$

and

$$(dC_O/dt)_{des} = (dC_C/dt)_{des} = 3.80\cdot10^4(A/V)\exp(-47500/T)(C_{Ce}C_{Oe} - C_C\,C_O)$$

CHAPTER 1
INTRODUCTION

A unique combination of properties such as relatively low density, high melting point, high superconducting transition temperature, low thermal neutron absorption cross section and good fabricability makes niobium and its alloys attractive candidate materials in a variety of applications. Its use ranges from superconductors, to high temperature structural applications, and to core materials for nuclear fusion reactors. However, because of the great affinity of Nb and niobium base alloys for interstitial elements like H, N, O, and C, these materials react readily with the reactive gases containing the interstitials causing striking changes in their physical and mechanical properties[53Ang, 63Des, 66Wis, 70Els, 71Mey 72Szk, 73Kle, 73Gin, 81Eng]. For example, 1 at.% nitrogen(= 0.15 wt%) dissolved in niobium increases its hardness by about 270% and its electrical resistivity by about 30%(Fig. 1.1)[63Geb, 66Geb]. The effects of interstitials on various properties of pure Nb are summarized in Table 1. Therefore, a strict control of the interstitial content is important for the reliable use of these materials in advanced technological applications.

Conventional production route of high purity Nb consists of (1) the extraction of Nb_2O_5 from niobium ores through leaching or chlorination/distillation (2) carbothermic or aluminothermic reduction of Nb_2O_5, (3) consolidation process to form the electrodes through sintering or remelting of Nb powder, and finally (4)

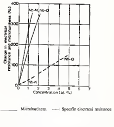

Fig. 1.1 Effect of dissolved gases on the mechanical and electrical properties of recrystallized niobium[63Geb, 66Geb]

Table 1 Property changes of Nb due to 1 at.% dissolved H, N, O, and C at ambient temperature *

specific property changes	Nb - H	Nb - N	Nb - O	Nb - C
Lattice parameter increase $\Delta a/\Delta c$, nm/at.%	2.3x10^{4}	6.0x10^{4}	6.1x10^{4}	
supplementary electrical resistance, $\Delta\rho/\Delta c$ $\mu\Omega$cm/at.%	0.66	4.1	4.1	4.3
Magnetic susceptibility decrease $\Delta\chi/\Delta c$, cm^3/g at.%		5.3x10^{4}	5.7x10^{8}	
Hardness increase, Vickers hardness number per 1 at.%	6.9	180	120	–
Hardening coefficient $\Delta\sigma/\Delta c$, MN/m^2 at.%	-	591	382	

* after ref.[80Fro, 81Sch1]

refining through electron beam remelting in vacuum [81Sch, 85Asf, 85Sch]. Among the above 4 stages, purification of Nb is mostly achieved during electron beam remelting in vacuum (EBM) and, in part, during consolidation step in high vacuum through degassing of nonmetallic elements and volatilization of metallic impurities.

In EBM, the electron beam, accelerated in a high potential, is focussed on to the Nb ingot to be melted, which drips down into a water cooled mold. The solidified ingot is then withdrawn downward on a base of the same material. Since this process is performed in high vacuum, non metallic impurities such as H, N, O, and C, and volatile metallic impurity like Al are removed to a great extent via degassing and vaporization process. Table 2 shows the typical impurity concentrations before and after EBM. In some cases, a special purification stage such as electrolytic refining in molten salt can be incorporated before EBM in order to eliminate the less volatile elements like Ta and W. On the other hand, Nb in solid state can be purified in ultra high vacuum at high temperature above 2000 °C, but purification kinetics is much slower than that in liquid state because transport from the interior to surface in solid state obeys the law of diffusion while in liquid metal transport of impurities take place via hydrodynamic flow. For example, it is reported by K. Schultz and et al. [81Sch1, 81Sch2] that an annealing time longer than one week is required to reach the ppm level for a niobium rod of 10 mm diameter at 2400 K under the nitrogen partial pressure of $5 \cdot 10^{-11}$ mbar. Thus, EBM has been used widely in the industries as a major purification step in the production route for high purity niobium since 1950s.

Table 2 Typical purity of niobium before and after electron beam melting*

atmosphere	$3 \cdot 10^{4}$ mbar
ingot diameter	125 mm
ingot melting speed(kg/h)	8 25(1st run) 12 85(2nd run) 59 (3rd run)

unit, ppm

Element	ATR** ingot	1st run	3rd run
H	< 50	20	8
N	40 – 1000	95	30
O	23000 45000	1800	130
C	500	70	40
Mo	< 10	< 10	< 10
Fe	4000 1000	80	< 10
Ni	10	< 10	< 10
Al	5000 14000	300	< 10
Si	> 1000	250	50
Ti	10	< 10	< 10
Zr	ND***	ND	ND
Ta	1450	1450	1450
W	40	40	40

* after ref [81Sch1]

** ATR Aluminothermic reduced

*** ND None detected (<< 10 ppm)

The first fundamental results concerning Nb and gas reactions at high temperature and low pressures were reported around 1965[65Pro1] Since then, a considerable amount of research has been carried out to understand the interaction behavior of interstitials in Nb but, in most cases, limited to the solid state. The high melting point of Nb (2468 °C) precludes the use of the conventional experimental techniques used to study such processes As a result, there is, at present, quite a lack of fundamental understanding of the interaction processes occuring between the gas phase and liquid Nb, which is essential for efficient refining and control of the interstitial content in the melt

The aim of this research is to attain a comprehensive understanding of mechanisms and kinetics of absorption and desorption behaviors of N, C, O in liquid Nb. The emphasis of the study is to determine the solubilities of each interstitial in liquid Nb, reaction mechanisms, rate controlling step, and rate equations.

The limitations of conventional techniques were circumvented in this study by carrying out the experiments in an electromagnetic (EM) levitation apparatus [65Fro3 65Pei, 84Eth] Electromagnetic levitation is particularly suited for the present study since this containerless processing method minimizes impurity pick-up from extraneous sources Also, the high melting temperature of Nb is not a serious constraint. Furthermore, the system offers the advantages of rapid heating under various gas atmospheres followed by rapid quenching if desired The sample can be cycled through desired temperature ranges for long periods of time, thus offering a way to monitor the interaction process under various processing conditions

CHAPTER 2
REVIEW OF LITERATURE

When a metal comes in contact with a gas phase, one of three possible reactions takes place depending upon the partial pressure of the gas. Those are (1) an absorption reaction in which the gas dissolves in the metal, increasing the concentration of gas species in metal, (2) a desorption reaction in which the gas species come out from the interior of the metal, resulting in the decrease of concentration of gas species in the metal, and (3) equilibrium in which apparently a reaction does not take place because the absorption rate is the same as desorption rate. In order to predict which reaction will occur under a given processing condition, it is necessary to compare the chemical potential of the species of concern in the metal and the gas atmosphere surrounding it. The interaction occurs in such a way so as to equalize the chemical potential of the species in both phases as a consequence of transfer of gas species from one phase to another.

In addition to the determination of the reaction direction based upon thermodynamic information, the next concern is how fast the reaction occurs and what mechanisms are controlling the overall reaction. Such information is essential for the determination of the reaction time to obtaining the desired level of interstitial content in the metal, the rate controlling step, and the processing parameters affecting the actual reaction rate.

In recent commercial Nb production lines, purification of niobium is mostly conducted by EBM in high vacuum Since the reduction of interstitial impurities in this stage is achieved through the gas-metal reaction at high temperature and low gas pressure thermodynamics and kinetics studies associated with it are both important to understand the purification process. Thermodynamics gives the information not only of the direction of reaction but also of the final composition attainable under a given processing condition Kinetic data will provide the idea of how fast the reaction can reach the equilibrium and how reaction rate can be adjusted toward the desired direction

Therefore, in the sections to follow, the thermodynamics associated with gas-metal reactions will be discussed first, followed by the discussion of mechanism and kinetics involved

Thermodynamics of Solution

When a metal reacts with gases such oxygen, nitrogen and CO, it depends upon temperature and partial pressure of the gas whether the reaction leads to the compound formation such as oxides, nitrides, and carbides, or to the interstitial solution in metal Below the dissociation pressure of the compound at a given temperature, the gas species are dissolved in metal in the form of interstitial solution, whereas beyond that pressure compounds start to form on the surface of metal. Discussion will be started with solution reaction

Suppose that a pure metal is in equilibrium with its vapor as follows,

$$M_{ss} \quad = \quad M_{gas} \qquad (2\ 1)$$

The free energies of the two phases in equilibrium are

$$G_M = G_{gm} \tag{2.2}$$

where G_M and G_{gm} are the free energies of a metal and its vapor, respectively. For a constant temperature the change in free energy of vapor phase due to its pressure change is calculated using the following equation.

$$dG_T = VdP_T \tag{2.3}$$

where V is the volume of the metal vapor and P is the vapor pressure. Integration of equation(2.3) gives

$$G_{gm} = G_{gm}^\circ + RT \ln (P_e/P_e^\circ) \tag{2.4}$$

where P_e is the equilibrium vapor pressure, **R** is the gas constant, **T** is the temperature, and ° indicates the properties at standard pressure. If the pressure is given in atm and the standard state is taken 1 atmosphere, the free energy of vapor pressure is

$$G_{gm} - G_{gm}^\circ + RT \ln P_e \tag{2.5}$$

On the other hand, for the metal, the free energy is given by

$$G_M = G^\circ_M \tag{2.6}$$

because the change in free energy caused by the change in pressure is negligible. According to equation(2.2), it can be seen that

$$G_M = G^\circ_M = G_{gm} = G^\circ_{gm} + RT \ln P_e \tag{2.7}$$

The change in the free energy due to vaporization is therefore

$$G^\circ_{gm} \quad G^\circ_M = \Delta G^\circ = \quad RT \ln P_e \tag{2.8}$$

This equation shows how the standard free energy change for vaporization is related to the equilibrium vapor pressure.

So far only equilibrium between a pure metal and its vapor has been considered. However, in many metallurgical processes metallic solutions of several components are usually involved. Thermodynamic treatment of these solutions is dealt with the partial free energy, which is defined as the change in the free energy of the solution when one mole of a substance is dissolved in a very large amount of solvent. In discussion regarding the equilibrium between pure metal and its vapor pressure, it was shown how the free energy of the gas or vapor phase is varied depending upon the change of pressure from P_a° to P_a. In a similar manner the change in the free energy of solution when one mole of substance i is added can be derived by substitution of the partial pressure P_i and P_i° for P_a and P_a°, respectively, leading to the following expression.

$$\Delta G = G - G_i^\circ = RT \ln (P_i/P_i^\circ) = RT \ln a_i \qquad (2.9)$$

where G and P_i are the free energy and partial pressure of substance i, respectively, and G_i° and P_i° indicate the same properties at standard state, respectively. The ratio P_i/P_i° is called the activity of substance i, a_i, in the solution. If X_i is the molar fraction of the component i in the solution, the following relation exists between its activity and the concentration X_i

$$a_i = \gamma_i X_i \qquad (2.10)$$

where γ_i is the activity coefficient of element i. Equation(2.9) becomes therefore

$$\Delta G = RT \ln \gamma_i + RT \ln X_i \qquad (2.11)$$

For an ideal solution, $\gamma = 1$, $a_i = X_i$. Such a solution has no interactions of the components, obeying Raults law. If $\gamma_i > 1$, there is a tendency for separation between solute and solvent atoms and a reduced solubility is observed for a given partial pressure of component i. Finally, if $\gamma_i < 1$, then there is a tendency for compound formation between the solvent and dissolved substance and a higher solubility is found than an ideal solution. Regarding the temperature dependence of the activity coefficient, temperature increase of a non-ideal solution, in principle, results in a decrease in the extent to which the activity coefficient deviates from ideal solution. In other words, if $\gamma_i > 1$, then an increase in temperature decreases the value of γ_i toward unity, increasing the solubility at a given partial pressure, whereas if $\gamma_i < 1$, then the value of γ_i increases toward unity with increasing temperature, resulting in the reduced solubility. It can be therefore predicted that if γ is greater than unity, the solution reaction is endothermic, while if γ_i is less than unity, it is exothermic.

Now, turning the attention to a dilute solution, it should be noted that there always exists a composition range with a constant activity coefficient, γ. If the constant value of the activity coefficient is set to be γ^{0}, the partial pressure of substance i can be written as

$$P_i = P^{0}_{i}\, a_i = P^{0}_{i}\gamma^{0}_{i} X_i = k_H X_i \tag{2.12}$$

which is the Henry's law and k_H is Henry's constant. Fig. 2.1 shows a typical diagram of the partial pressure of the components of a binary alloy system with positive deviation. When Rault's law is obeyed, the partial pressure is linearly proportional to molar fraction, lying on the straight lines. Henry's lines are the tangents to the activity curve for X_A or $X_B > 0$ respectively. As may be seen from the diagram, γ_A and γ_B are constant only over a very small range of concentration. The partial pressure curves also demonstrate that Rault's law is obeyed for the solvent.

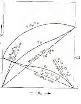

Fig. 2.1 Examples of the relationship between vapor pressure and concentration in a binary system A B with a positive deviation from Rault's Law [71Win2]

In many gas-metal systems, the solubility is so low that it is usually not convenient to refer to the pure substance as "standard state." More often, the Henry's activity based on Henry's line, a^H, is used, which is defined as

$$a_i^H = f_i\ C_i \tag{2.13}$$

where Henrian activity coefficient, f_i, becomes unity when the concentration of the specie i, C_i -> 0. The concentration C_i is conventionally expressed in weight %. Henry's activity a_H, is therefore equal to the concentration of the dissolved substance C_i in weight % in ideal dilute solutions

Solubility of Gases in Metals

Since most of gases are dissolved in metals almost solely in their atomic state the solution reaction, for instance, for nitrogen can be represented as

$$1/2\ (N_2) = [N]_M \tag{2.14}$$

with the equilibrium constant,

$$K = \frac{a_N}{(P_{N_2})^{1/2}} = \frac{f\ C_N}{(P_{N_2})^{1/2}} = \exp(\ -\Delta G^\circ/RT) \tag{2.15}$$

where a_N is the activity of nitrogen P_{N_2} is the partial pressure of N_2, f is the Henrian activity coefficient, C_N is the nitrogen concentration, ΔG° is the free energy change for solution reaction of one mole of nitrogen atom, R is the gas constant, and T is the temperature. For low concentrations where the activity coefficient is almost constant, solubility, C_N, is proportional to the square root of partial pressure, $P_{N_2}^{1/2}$, for diatomic gases. This is the well known Sievert's law and can be expressed as

$$C_N = k(T)\ (P_{N_2})^{1/2} \tag{2.16}$$

where k(T) is temperature dependent Sieverts constant. From the equation (2.15), the following relationship can be derived as

$$C_S = (1/f)\,(P_{S_2})^{1/2} \exp(-\frac{\Delta H^\circ}{RT} + \frac{\Delta S^\circ}{R}) \qquad (2.17)$$

where ΔH° and ΔS° are solution enthalpy and entropy change, respectively. Hence, f is unity in dilute solutions where Henry's law is valid and standard state is taken as 1 wt.% solution. Therefore, comparing equation(2.16) with (2.17), it can be seen that

$$k(T) = \exp(-\frac{\Delta H^\circ}{RT} + \frac{\Delta S^\circ}{R}) \qquad (2.18a)$$

or

$$\ln k(T) = -\frac{\Delta H^\circ}{RT} + \frac{\Delta S^\circ}{R} \qquad (2.18b)$$

Substituting the equation (2.18b) into equation (2.16), it is found that solubility, C_S, is related to the partial pressure and temperature as

$$\ln C_S = \frac{\Delta S^\circ}{R} - \frac{\Delta H^\circ}{R}\frac{1}{T} + \frac{1}{2}\ln P_{S_2} \qquad (2.19)$$

Equation (2.19) indicates that the solubility at a constant pressure is increased with rising temperature if ΔH° is positive, i.e., if the solution reaction is an endothermic process, while the solubility is decreased with the increase of temperature if ΔH° is negative, i.e., if the solution reaction is exothermic. On the other hand, the solubility at a given temperature is increased with increasing partial pressure.

In practical application of solution reaction of the interstitials in metal such as vacuum degassing, it is necessary to examine how the solubility varies with the change of partial pressure and temperature. Fig. 2.2 shows the pressure dependence of the solubility of various gases (also those of sulphur and phosphorous) in the

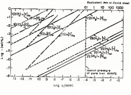

Fig 2.2 Solubilities of gases in liquid iron at 1600 °C, in liquid nickel at 1450 °C and liquid chromium at 1745 °C [71Wis2]

liquid iron, nickel, and chromium [71Win2]. It may be seen that only for hydrogen and nitrogen, the equilibrium pressures are high enough even at low concentrations that a vacuum removal of the elementary gases is feasible by lowering the pressure. This fact is quite important in vacuum degassing because degassing is possible without a significant loss of metal only when sufficiently high molar concentrations of the gas exists in the vapor coming out from the metal.

Fig. 2.3 shows the temperature dependence of equilibrium pressures of oxygen at a given oxygen level of 100 ppm for iron, nickel, and copper. The slope of these curve is markedly smaller than that of the vapor pressure curves of the solvents. It may therefore be predicted that no improved degassing conditions can be obtained for oxygen by raising the temperature.

Temperature dependence of the solubility of gases varies greatly from metal to metal. Fig. 2.4 shows the nitrogen solubilities in group Vb(Ta, Nb) and VIb(W, Mo, Cr) solid metals. Solid lines indicate the solubility lines whereas dot-dashed lines represent the phase boundary between a solid solution and compounds. With increasing the temperature, nitrogen solubilities increase for VIb metals but decrease for Vb metals. This indicates that the solution reaction for Nb and Ta is exothermic(ΔH negative) whereas, for group VIb metals, it is endothermic(ΔH positive). At temperatures between 1600 and 2400 °C, niobium and tantalum show rather high nitrogen solubilities(between 0.1 and 10 at%) at relatively low nitrogen pressure of 10^{-4} to 1 torr. The terminal solubility(dot-dashed lines) of several at% can easily be reached at temperatures of about 2000 °C and below. In contrast, the nitrogen solubility in Mo, W, or Re is very low(10^{-3} at%) even at pressures of about

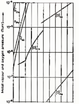

Fig 2.3 Temperature dependence of the oxygen pressure of copper, iron, and nickel containing 100 ppm oxygen and of the vapor pressure of the pure metals.[71Wm2]

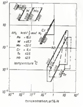

Fig. 2.4 Solubilities of nitrogen in solid Nb, Ta, Cr, Mo, W and Re [72Fro1]

1 atm N_2. Based on those facts, it can be stated that degassing treatments in vacuum are most effective for group Vb metals at very high temperatures whereas for group VIb metals the annealing temperatures should be low as far as kinetic consideration allows.

For oxygen, solid solution as a rule, is expected only in very low concentration ranges because of higher affinity to metal compared with that of hydrogen or nitrogen. In such a limited composition range the deviation from Henry's line is usually very small, as demonstrated in Fig. 2.5, in which solubility of oxygen in iron, nickel, and their alloys is plotted. In addition, the maximum attainable equilibrium pressure for a given temperature corresponds to the decomposition pressure of the oxide, which is in equilibrium with the melt at saturation. Therefore the terminal solubility of gas atom in the solid or in the liquid can be determined by thermochemical stability of oxides with respect to the solution phase. Consider the reaction of oxide formation for the metal-oxygen reaction as

$$1/2\ O_2(g) + mM \rightarrow M_mO \qquad \Delta G^\circ \tag{2.20}$$

and the solution reaction as

$$1/2\ O_2(g) \rightarrow O(\text{in } M) \qquad \Delta G_1^\circ \tag{2.21}$$

The equation for the oxide formation from saturated solution is derived by subtracting equation (2.20) from equation (2.21)

$$M_mO \rightarrow O(\text{in } M) + mM \quad \Delta G_2^\circ \tag{2.22a}$$

or

$$\Delta G_2^\circ = \Delta G_1^\circ - \Delta G^\circ \tag{2.22b}$$

Equilibrium constant for reaction (2.22a), Kp, is given by

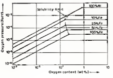

Fig. 2.5 Oxygen pressure as a function of the oxygen content of pure iron, pure nickel and several iron-nickel alloys at 1600 °C [60Win]

$$Kp = a_O = C_O = \exp(-\Delta G_1^\circ/RT) \tag{2.23}$$

where **R** is the gas constant and **T** is the temperature. Accordingly, the terminal solubility, $C_{O,max}$, in the dilute solution yields

$$\ln C_{O,max} = -\frac{\Delta G_1^\circ}{RT} = -\frac{\Delta H_1^\circ}{RT} + \frac{\Delta S_1^\circ}{R} = A + \frac{B}{T} \tag{2.24}$$

where ΔH_1° and ΔS_1° are the enthalpy and the entropy for oxide formation from saturated solid solution, respectively. This equation shows the temperature dependence of terminal solubility.

Deoxidation by Reduction Processes or by Evaporation of Suboxides

As mentioned previously the oxygen partial pressures in equilibrium with refractory metals and their alloys containing oxygen impurity are so low that it should generally be expected that in ordinary vacuum a pick-up of oxygen from residual gas atmosphere occurs rather than a removal. Therefore, in many cases the deoxidation of refractory metals are performed via the reduction by carbon or hydrogen, and the suboxide vaporization.

Reduction by Carbon or Hydrogen

The deoxidation of refractory metals can be achieved by the use of carbon which, particularly under reduced pressures, has a very high affinity for oxygen. The principal reaction governing oxygen removal by carbon is the formation of carbon monoxide as

$$[C]_M + [O]_M = CO(g) \tag{2.25}$$

where $[C]_M$ and $[O]_M$ are, respectively, carbon and oxygen dissolved in the metal. Fig. 2.6 shows the vapor pressures of pure Nb, Nb-O, and Nb-C-O solid solutions.

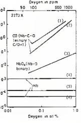

Fig 2.6 Equilibrium vapor pressure over the Nb-O and Nb-C O solid solutions at 2273 K [80Ono] Vapor pressure lines are taken after line(1)[68Fro2], line(2)[77Ued], lines(3) and (4)[64Geb], line(5)[59Spe], and line(6)[36Ref]

with up to 1 at% O at 2273 K. A comparison of vapor pressures of Nb-O and Nb-C-O solid solutions indicates that CO pressure in equilibrium with Nb-C-O solution is roughly two orders of magnitude greater than NbO_x vapor pressure at the same oxygen level. This implies that deoxidation due to CO degassing is much more effective than that due to niobium oxide evaporation which will be described later.

On the other hand, the deoxidation by hydrogen is done according to the reaction following equation

$$[O]_{Nb} + H_2(g) = H_2O(g) \tag{2.26}$$

with the equilibrium constant, K:

$$K = P_{H_2O}/(a_O P_{H_2}) \tag{2.27}$$

This reduction process is of particular interest for cases where the reduction by carbon cannot be carried out because of the formation of stable carbide. It can be seen that the higher the ratio of P_{H_2}/P_{H_2O} is the more effective the deoxidation is.

Deoxidation by Evaporation of Suboxides

In some metal-oxygen systems, high vapor pressure of oxides can be utilized successfully for deoxidation. One of those systems is Nb-O system. In vacuum degassing of Nb containing oxygen impurity, the low equilibrium oxygen partial pressure of solution eliminates the possibility of oxygen removal through the direct oxygen molecule degassing. Instead, the evaporation of Nb suboxides may lead to the decrease of oxygen level. When niobium is annealed in vacuum, some of the oxygen striking the surface of Nb evaporates back into vacuum in the form of suboxides while some others are dissolved in Nb. Since the oxygen content in niobium increases with time at a given partial pressure of oxygen and desorption rate via volatile oxides increases with increasing oxygen content, a steady state is reached when the rate of oxygen removal due to oxide evaporation is equal to the rate of oxygen dissolution. At this condition, the oxygen concentration remains constant at a level corresponding to the given oxygen partial pressure and temperature. Oxygen concentration in solid Nb at steady state is reported to be lower as temperature increases or oxygen partial pressure decreases[66Hor1].

The possibility of deoxidation via volatile oxide evaporation can usually be examined using the evaporation ratio suggested by Brewer and Rosenblatt[62Bre], who developed the idea based upon the thermochemical stability of oxide. The definition of the ratio is given below

$$R = \frac{(\Sigma\ y\ P_{MxOy} / \Sigma\ x\ P_{MxOy})_{in\ gas}}{(N_O / N_M)_{in\ cond}} \tag{2.28}$$

where P_{MxOy} is the equilibrium partial pressure of volatile oxides being considered and N_O and N_M the molar fraction of oxygen and metal in the condensed phase. For favorable purification, it is recommended that R should be at least 10 or greater. Table 3 [62Ono] summarizes the equilibrium thermodynamic data concerning evaporation deoxidation and the calculated evaporation ratio, R, for several elements. The elements in group IV have a large solubility and lose oxygen as an MO species so that the value of R is small. The elements in group V lose oxygen as suboxides. Purification via suboxide vaporization could be practical for these elements except V-O system, where the vapor pressure of the base metal is relatively large. Chromium in group VI is not a good candidate because of the high vapor pressure of Cr itself. The refractory metals Mo and W of the group VI have extremely high R values, indicating very effective purification by vaporization. The major

Table 3 Thermodynamic data and evaporation ratios relating to the deoxidation of refractory metals in solid state *

Metal melting temp (K)	Temp (K)	Solubility limit of oxygen wt% (at%)	Activity coeff	Vapour pressure of the gaseous species: species	p_{MxOy}/P^0	Vapor pressure of the metals p/p^0	Evaporation ratio R
IV							
Ti (1943)	1800	13.6 (32)	1.4x10^{-15}	Ti TiO	5.2x10^{-8} 1.3x10^{-7}	6.0x10^{-7}	2
Zr (2130)	2000	7.3 (31)	–	ZrO ZrO$_2$	5.9x10^{-8} 7.0x10^{-11}	2.2x10^{-9}	2
Hf (2503)	2000	2.2 (20)	–	Hf HfO	4.8x10^{-10} 2.6x10^{-1}	1.9x10^{-8}	0.2
V							
V (2175)	1800	8.1 (22)		V VO	1.6x10^{-8} 3.6x10^{-5}	7.8x10^{-8}	4
Nb (2741)	2000	1.2 (6.8)	9.8x10^{-8}	NbO NbO$_2$	5.7x10^{-8} 4.4x10^{-7}	1.8x10^{-11}	28
Ta (3288)	1800	0.43 (4.7)	7.4x10^{-7}	TaO TaO$_2$	4.4x10^{-10} 1.4x10^{-4}	5.5x10^{-16}	42
VI							
Cr (2130)	1800	0.015(0.05)	9.6x10^{-4}	Cr CrO$_2$ CrO	1.9x10^{-5} 4.0x10^{-8} 3.7x10^{-4}	9.6x10^{-5}	3
Mo (2893)	2000	0.007 (0.04)	1.5	MoO$_3$ (MoO$_3$)$_3$ MoO$_2$	7.1x10^{-4} 3.6x10^{-4} 8.3x10^{-5}	2.3x10^{-16}	7350
W (3683)	1973	0.005 (0.06)	1.0	(WO$_3$)$_3$ (WO$_3$)$_4$ W$_3$O$_8$	0.29 0.078 0.066	1.7x10^{-13}	4900

* after ref [82Ono]   p is given in Pa and P^0=101325 Pa. R is the calculated value at $C_{O,sat}$

vaporization oxide species are MO_2 type molecules and its dimer. These metals are characterized by the small solubility and low activity of oxygen.

Phase Diagrams and Thermodynamic Data

Nb - N System

The Nb-N phase diagram is shown in Fig. 2.7. Up to 60 at% N, there are two nitride phases, Nb_2N, and NbN. Nb_2N has a hexagonal close packed structure and homogeneity range of 28.5 to 32.4 at% N. The NbN phase undergoes a transformation from face centered cubic to hexagonal close packed at approximately 1300 °C. The solubility of nitrogen in Nb, C_N, is given as a function of partial pressure of nitrogen and temperature by the following equations. For nitrogen solubility in α - Nb[68Fro1], it is

$$\log C_N = 1/2 \log P_{N_2} - 3.10 + 9300/T \ (1770<T<2470 \text{ K}) \qquad (2.29a)$$

and for N in liquid Nb[73Rev], it is given as

$$\log C_N = 1/2 \log P_{N_2} + 0.28 \ (< 15 \text{ at\%}, T = 2800 \text{ K}) \qquad (2.29b)$$

with P_{N_2} in mbar, T in K and C_N in at%. Some thermodynamic data associated with Nb-N system is summarized in Table 4.

The pressure-concentration isotherms are shown in Fig. 2.8 in which a slope of 2 for the region of α-solid solution implies that nitrogen is dissolved in atomic form in the solid solution. The kink of the isotherms in the lower regime of C_N gives the concentration at which niobium is saturated with nitrogen at the given temperature and also the subnitride phase, Nb_2N, starts to form. For constant N_2 pressures, the N concentration in the solid solution decreases with increasing

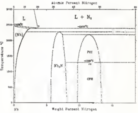

Fig. 2.7 Nb - N phase diagram.[81Sch1]

Table 4 Thermodynamic data associated with Nb + N system

Equilibria C in at%, P in torr, T in K	$\Delta G°$ in cal	References
$1/2(N_2) = [N]_{Nb}$		
$\log C_N = 1/2\log P_{N_2} + 3.1 + 9300/T$ (1730 - 2470 K)	$-42500 + 16.8T$	[68Fro1]
$^*\log C_N = 1/2\log P_{N_2} + 0.22$ (T = 2800 K, < 15 at%)		[73Rev]
$2<Nb> + 1/2(N_2) = <Nb_2N>$ (1730 - 2470 K)		
$\log P_{N_2} = 12.6 + 28400/T$	$65100 + 22.2T$	[68Fro1]
$<Nb_2N> = 2<Nb> + [N]_{Nb}$ (1730 - 2470 K)		
$\log C_N = 3.17 - 4920/T$	$+22500 - 5.35T$	[68Fro1]

* Solubility in liquid phase and P in mbar

( ) gas phase, [ ] interstitial in solid solution, and < > solid phase.

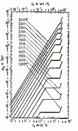

Fig. 2.8 Pressure - concentration isotherm in Nb - N system [66Geb]

temperature. The other kink in each isotherm indicates the concentration at which nitrogen starts to dissolve in Nb_2N in the form of solid solution. In Fig. 2.9, the solubilities in niobium at 2050 °C just below and above its melting point are plotted against the N_2 partial pressure. It is seen that at the given N_2 pressure more amount of nitrogen is dissolved in the melt than in solid.

Nb – O System

The Nb – O phase diagram is shown in Fig. 2.10. Three different oxides exist, NbO, NbO_2, and Nb_2O_5. The melting points of the oxides are 1945, 1925, and 1495 °C respectively. The maximum solubility of oxygen in α-Nb is 7.5 at.% at 1915 °C. The O_2 equilibrium pressure over the α solid solution is so low that direct measurements of the solubility data cannot be performed even under high vacuum. Instead, the equilibrium data can be obtained from the temperature dependence of the terminal O solubility and ΔG° values of oxide formation. The solubility in α-solid Nb is given by equation[68Fro1]

$$\log C_O = 1/2 \log P_{O_2} - 4.45 + 20020/T \qquad (2.30)$$

($1570 < T < 2270$ K), with P_{O_2} in mbar, T in K and C_O in at. %

The terminal solubility C_{Omax} in α-Nb is given as[68Fro1]

$$C_{Omax} = 1.67 - 1680/T, \ (1070 < T < 1770 \text{ K}) \qquad (2.31)$$

The vapor pressure of the volatile oxides over Nb containing O were determined to be[68Fro1]

$$\text{NbO(g)} \quad \log P_{NbO} = \log C_{O \text{ in Nb}} + 9.12 - 28400/T \qquad (2.32a)$$

$$(1870 < T < 2470 \text{ K}),$$

and

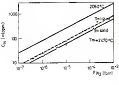

Fig. 29 Nb - N system, log P – log C_N diagram at the melting point of Nb [81Scb1]

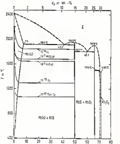

Fig 2.10 Nb - O phase diagram.[60Ell, 68Fro1]

$NbO_2(g)$ $\quad \log P_{NbO_2} = 2 \log C_{O\ in\ Nb} + 7.12 - 24300/T$ (2.32b)

(1870 < T< 2470 K)

Thermodynamic data concerning Nb-O system are summarized in Table 5. The pressure - concentration isotherms for the steady states of niobium annealed in O_2 is plotted logarithmically in Fig. 2.11[77Sch]. The isotherm shows a slope of 1 at constant temperature $C_o \propto P_{O_2}$. Evaporating species consists of two oxides NbO and NbO_2, and NbO is a predominant at lower concentration and higher temperatures. The percentage of NbO is indicated by dot-dashed lines. The existence of steady state is restricted to the region of the α solid solution limited by the solvus and solidus lines (dotted and dashed lines in the upper part of the graphs). Furthermore, at low temperatures the steady state conditions cannot be realized any longer due to the negligible oxide evaporation leading to a continuous oxygen absorption and oxide scale formation. Only at very low O_2 pressure is a steady state still available, but due to the extremely low reaction rate, very long period is necessary. The oxygen concentration in the steady state condition is found to be related to the oxygen partial pressure and temperature as follows[77Sch]:

$$C_o = P_{O_2} \cdot 9.1 \cdot 10^{8} \ \exp(\ 502000/RT) \qquad (2.33)$$

(2170 < T < 2540 K)

where C_o is in at.% and P_{O_2} in mbar, and R is 8.31 J/mol K.

This equation can be utilized to estimate the residual oxygen content after annealing treatments. On the other hand, it should be mentioned that in contrast to true equilibrium, an additional metal loss always appears in steady state due to the constant oxide evaporation rate which can be larger by several orders of magnitude

Table 5 Thermodynamic data associated with Nb O system.

Equilibria C in at% P in torr T in K	ΔG° in cal	References
$1/2(O_2) = [O]_s$		
$\log C_o = 1/2 \log P_{O_2} - 4.5 + 20200/T$	$-92300 + 23.0T$	[68Fro1]
$1/2(O) = [O]_s$		
$\log C_o = 1/2 \log P_O - 9.4 + 33400/T$	$-152900 + 39.0T$	[68Fro1]
$(NbO) = [O]_s + \langle Nb \rangle$		
$\log C_o = \log P_{NbO} - 9.0 + 28400/T$	$13000 + 37.1T$	[64Fro1]
$1/2(NbO_2) = [O]_s + 1/2\langle Nb \rangle$		
$\log C_o = 1/2 \log P_{NbO_2} - 3.5 + 12150/T$	$55500 + 18.5T$	[68Fro1]
$\langle Nb \rangle + 1/2(O_2) = \langle NbO \rangle$		
$\log P_{O_2} = 12.3 - 43700/T$	$-100000 + 21.5T$	[68Fro1]
$\langle Nb \rangle + (O) = \langle NbO \rangle$		
$\log P_O = 11.1 - 35100/T$	$160600 + 37.5T$	[68Fro1]
$\langle NbO \rangle = \langle Nb \rangle + [O]_s$		
$\log C_o = 1.67 - 1680/T$	$+7700 + 1.5T$	[72Fro1]
Steady state		
O_2 $\log C_o = \log P_{O_2} - 3.35 + 16700/T$		[69Fro1]

( ) gas phase, [ ] interstitial in solid solution, and < > solid phase.

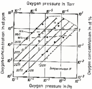

Fig. 2.11 Steady state during annealing of Nb in O_2 atmosphere.[77Sch]

than metal evaporation rate, as can be seen from Fig. 2.12[69Fro, 70Fro1]. The evaporation rate is given by the thickness decrease of base metal per hour in μm/h. It can be seen that, in the pressure-temperature range of steady state, NbO and NbO_2 gases are predominant evaporating species. However, at very high temperature and the low pressure region, it is possible for the pure metal evaporation to exceed the oxide evaporation.

Nb - C system

The Nb- C phase diagram is shown in Fig. 2.13. There exists two carbide phases, namely, hexagonal close packed Nb_2C and NaCl-type cubic NbN. The maximum solubility of carbon in α-Nb is 3.5 at.% at about 2300 °C. In the Nb-C system only the terminal solubility of the α solid solution can be determined as a function of temperature as follows:

$$\log C_c = 3.65 - 7600/T \quad (1770 < T < 2470\ K) \tag{2.34}$$

During annealing of niobium in CO atmospheres, thermodynamic equilibrium is established according to the reaction,

$$(\,CO\,)_g \;=\; [O]_{ss} + [C]_{ss} \tag{2.35}$$

The CO pressure over Nb-C-O solid solutions are given by the following expression [68Fro2]

$$\log P_{co} = \log C_c + \log C_o + 6.32 - 14700/T \tag{2.36}$$

(1870 < T < 2170 K) with P_{co} in atm and C_c and C_o in at%

Other thermodynamic data on Nb-C system is given in Table 6

In Fig. 2.14, experimentally determined CO equilibrium pressure isotherms for Nb-C-O solid solution with the concentration ratio C/O =1 are graphically shown

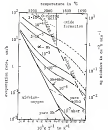

EVAPORATION RATES OF Nb in O_2
ATMOSPHERES AS A FUNCTION OF 1/T.
T-p RANGES FOR STEADY STATES.

Fig. 2.12 Evaporation rates of Nb in O_2 [69Fro]

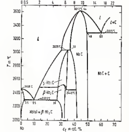

Fig. 2.13 Nb – C phase diagram.[81Sch]

Table 6 Thermodynamic data associated with Nb - C system.

Equilibria C in at% P in torr, T in K	ΔG^{0} in cal	References
$<C> = [C]_s$		
	3100 9.5T	[64Geb]
$2<Nb> + <C> = <Nb_2C>$		
	37900 - 2.0T	[68Fro1]
$<Nb_2C> = 2<Nb> + [C]_s$		
$\log C_s = 3.65 - 7600/T$	+34800 7.53T	[66Geb]
$(CO) = [C]_s + [O]_s$		
$\log P_{co} - \log C_c \ \log C_o = 6.2 - 14700/T$	67000 + 33.5T	[68Fro1]
$1/2(O_2) + <C> = (CO)$		
	28400 20.0T	[68Fro1]

( ) gas phase, [ ] interstitial in solid solution and < > solid phase

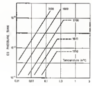

Fig. 2.14 Equilibrium pressure of CO over Nb-C-O solid solution with the ratio of C to O equal to unity [76Fro]

on a logarithmic scale. Equilibrium C or O concentration at a given partial pressure of CO decreases with increasing temperature, indicating that CO dissolution in Nb is an exothermic reaction. The CO equilibrium pressure over solid solution of C and O containing a fraction of at% at 2000 to 2600 K is relatively high, making it possible for reaction(2.35) to be used for removing carbon from niobium by a high vacuum treatment. For a given partial pressure of CO, $C_c \cdot C_o$ is constant at a constant temperature. Therefore, carbon can be removed by annealing the specimen in O_2 atmosphere.

Reaction Rate

The rate of reaction is formally defined as the change in moles of a component per unit volume with respect to time. The mathematical expression for the rate, r, is

$$r = \frac{1}{V}\frac{dN}{dt} = \frac{dC}{dt} \tag{2.37}$$

where V, N, and C are the volume, the number of moles, and the molar concentration of the species involved in the reaction. If the stoichiometric coefficients for two reactants are different, the rate expressed in terms of one reactant will not be the same as the rate expressed in terms of the other. Consider the following reaction

$$aA + bB \rightarrow cC + dD \tag{2.38}$$

The concentration changes for the four reactants and products are related as follows

$$r = -\frac{1}{a}\frac{d[A]}{dt} = -\frac{1}{b}\frac{d[B]}{dt} = \frac{1}{c}\frac{d[C]}{dt} = \frac{1}{d}\frac{d[D]}{dt} \qquad (2.39)$$

where [A] is the concentration of reactant A, etc.

In order for reaction to take place, each reactant should be close enough to make collision. Therefore, the reaction will be proportional to the frequency of collision which, in turn, is associated with the concentration of each species in the following way:

$$-\frac{1}{a}\frac{d[A]}{dt} = \frac{1}{c}\frac{d[C]}{dt} = \mathbf{k}\ [A]^{n}\ [B]^{m} \qquad (2.40)$$

where n and m are the order of reaction with respect to [A] and [B] respectively, and k is the rate constant. The sum of n and m is called the order of the overall reaction. The order and the stoichiometric coefficients in the reaction equation are not necessarily interrelated, i.e., it is not required that n=a and m=b. In general, the order is determined experimentally. Since concentration data is in practice, measured as a function of time, the integral form, rather than the differential form, of reaction rate equation is more frequently used in determining the order of reaction because data can be plugged into it directly.

Rate Controlling Step

As shown in many kinetics studies, the formation of the final products from the original reactants usually occurs in a series of relatively simple steps which may be physical or chemical in character. In order to understand the gas-metal reaction in terms of kinetics it is important to consider the reaction mechanism which is the sequence of steps that describe how the final products are formed from the original reactants. The rate of the individual steps will normally be different, and the rate of the overall reaction will be determined primarily by the slowest among these steps. Herein lies the explanation for the difference between the order of reaction and the stoichiometric coefficients. Together with the reaction mechanism, it is also important to understand the concept of rate controlling step. While the notion of "bottle neck" process in a series of subprocess is intuitively obvious, it is often carelessly applied or stated. Since a clear understanding of the implication of a rate controlling or the slowest step is central to the correct interpretation of coupled physical and chemical reaction phenomena, the concept of rate controlling step motivated by C. Wagner[70Wag] will be mentioned below.

Consider a sequence of consecutive steps of a reaction involving species, A as the reactant, Z_1, Z_2, • • • as the intermediates, and species B as the product.

$$A \overset{I}{=} Z_1 \overset{II}{=} Z_2 \overset{III}{=} \cdots \overset{n}{=} B \tag{2.41}$$

where steps are numbered by I, II, • • • ,n. Since the concentrations of the intermediates are small in comparison to those to A and B, after a relatively short induction period, a steady state with virtually equal net rate, v_I, v_{II} • • • of the individual steps is established. Thus, the net rate v, of the overall reaction A → B is

$$v = v_I = v_{II} = \cdots = v_n \tag{2.42}$$

The above statement is not consistent with the general definition of rate determining step and therefore must be modified. This is possible by introducing the concept of the virtual maximum rate v_i^*, of each individual step. The virtual maximum rate is defined as the rate which would be observed if for all steps other than step i virtual equilibrium were established, e.g. with the help of appropriate catalysts (and all other irreversible steps were comparatively fast). Then the concentration C_{i-1}^* of species Z_{i-1} in the case of equilibrium for all steps preceding step i equals to

$$C_{i-1}^* = C_A (K_I K_{II} \cdots K_{i-1}) \tag{2.43}$$

where K_i denotes the equilibrium constant of step i. Furthermore the concentration of species Z_i in the case of equilibrium for all steps following step i is given by

$$C_i^* = C_B (K_{i+1} K_{i+2} \cdots K_n)^{-1} \tag{2.44}$$

The equilibrium constant K of the overall reaction, A = B is related to that of each step as follows

$$K = (K_I K_{II} \cdots K_n) \tag{2.45}$$

For each individual step, virtual maximum rate v_i^* is then given by

$$v_I^* = k_I C_A - k_I' C_I^* = k_I (C_A - C_I^*/K_I) = k_I (C_A - C_B/K)$$
$$v_{II}^* = k_{II} C_I^* - k_{II}' C_{II}^* = k_{II} (C_I^* - C_{II}^* / K_{II}) = k_{II} K_I (C_A - C_B/K) \tag{2.46}$$

$$\cdots\cdots\cdots\cdots\cdots\cdots$$

$$\cdots\cdots\cdots\cdots\cdots\cdots$$

$$v_n^* = k_n C_{n-1}^* - k_n' C_n^* = k_n (C_{n-1}^* - C_n^*/K_n) = k_n K_{n-1} K_{n-2} \cdots K_I (C_A - C_B/K)$$

where k_i and $k_i'(= k_i/K_i)$ indicate the rate constants of the forward and the backward reaction of step i respectively. On the other hand, if equilibrium for the individual steps is not established, it yields

$$v = k_I (C_A - C_I/K_I)$$
$$v = k_{II} (C_I - C_{II}/K_{II}) \tag{2.47}$$

$$\cdots\cdots\cdots\cdots$$

$$\cdots\cdots\cdots\cdots$$

$$v = k_n (C_{n-1} - C_n/K_n)$$

Dividing through corresponding side of equation (2.46) and (2.47) and adding the individual quotients, it yields

$$\frac{v}{v_1^*} + \cdots + \frac{v}{v_n^*} = \frac{C_A - C_B/(K_1 \cdots K_n)}{C_A - C_B/K} = 1 \qquad (2.48)$$

Thus,

$$v = \frac{1}{1/v_1^* + 1/v_2^* \cdots + 1/v_n^*} \qquad (2.49)$$

This equation implies that the observed reaction rate, v, inherits characteristics of the individual rates, v_i^*, and is practically equal to the virtual maximum rate v_j^* of step j if v_j^* is much less than the virtual maximum rates of all other steps.

$$v = v_j^* \qquad \text{if } v_j^* << v_{i\neq j}^* \qquad (2.50)$$

Therefore, it can be justified that the overall reaction rate, v depends only on the parameters governing v_j^* becoming insensitive to the characteristics of all of the other rate equations $v_i^*(i\neq j)$

Effect of Temperature on Reaction Rate

In deriving the rate equation dC/dt = k[A], the effect of concentration difference between the initial and the final states is directly incorporated into the concentration terms as a driving force for the reaction, but the influence of the other parameters is represented in the rate constant, k. Such parameters include the resistance to mass transfer in the gas phase or liquid phase, temperature, physical conditions of specimen such as surface to volume ratio and so on. The effect of barrier to the mass transport will be discussed later in detail. Temperature is one of the most important variables to be included in the rate constant, particularly for the interfacial elementary steps.

Temperature dependency of rate constant, k, for an elementary process obeys the Arrhenius equation. Thus, it is given by

$$k = k_0 \exp(-Q / RT) \tag{2.51}$$

where k_0 is a preexponential constant.

Q is the activation energy

R is the gas constant.

T is the absolute temperature.

Combining equation(2.51) and (2.40) yields

$$d[A]/dt = k_o \exp(-Q/RT) [A]^a [B]^b \tag{2.52}$$

It should be noted that this expression is rigorously limited to an elementary process because the Arrhenius equation is so restricted. However the exponential effect of temperature often accurately represents experimental rate data for an overall reaction, even though the activation energy is not clearly defined and may be a combination of Q values for several elementary steps.

The different value of activation energy for each elementary step leads to a different temperature dependence of each step, resulting in the switch of rate controlling step from one to another in different temperature regime. According to Fig. 2.15, the elementary step B with higher activation energy may be the slowest at low temperatures(shown by range a in the figure) and could well become rate determining for the total degassing reaction. On the other hand, at high temperatures(range c) the step C with lower activation energy is the rate

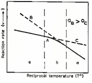

Fig. 2.15 Rate of a reaction(A) consisting of two partial reactions (B and C) which are both rate determining[71Win1]

determining. In the intermediate temperature range, b, both elementary steps proceed at about the same rate so that the whole reaction process becomes under control of both steps in a mixed mode.

Energetics of Reaction Path

In the earlier section it was discussed how the overall reaction is related to each elementary step and the overall reaction rate is associated with the individual substep reaction rates. In the following section, the relationship between the overall reaction and individual elementary steps will be discussed from the energetic point of view. For example, the energy diagrams for A_2 dissolution reaction are schematically illustrated in Fig. 2.16 where the energy of one mole A_2 or two g-atoms A is plotted against the distance of the molecules or atoms from the metal surface for two types of metal gas systems. Fig. 2.16(a) shows the energy change for a system with a large negative heat of solution ΔH° such as Nb-N, Ta-N, and V-N (Vb group – N) whereas Fig. 2.16(b) is for a system with a large positive value of ΔH° such as Cr-N, Mo-N, and W-N (VIb group – N). During gas dissolution, an A_2 molecule passes at first through a shallow potential minimum of molecular adsorption and reach the activated state for dissolution as A atoms. The A atoms are then chemisorbed, penetrate the metal surface, and diffuse in the bulk of the metal. During desorption the same steps are passed in the reverse direction. Q_{ab} and Q_{des} denote the apparent activation energies for absorption and desorption. Q_{chem}, Q_i, Q_s, and Q_{dif} are the true activation energies for dissociative chemisorption,

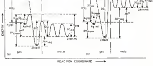

Fig 2.16 Energy diagrams for reversible absorption and desorption of diatomic gases A_2. ΔH_D dissociation energy, ΔH_{chem}, ΔH_s and ΔH_{seg} heat of chemisorption, solution and segregation, Q_{ab} and Q_{des} experimental activation energy of absorption and desorption, Q_{chem}, Q_1 or Q_s, Q_{diff} true activation energy of dissociative chemisorption, transfer through metal surface, and diffusion. [80Fro]

(a) exothermic solution reaction, (b) endothermic solution reaction transfer through the metal surface in absorption and desorption, and diffusion of A atom respectively ΔH° indicates the heat of solution.

The differences in reaction rates and activation energies for nitrogen absorption and desorption between group Vb metal and group VIb metals can be correlated with the different sign for the heat of solution ΔH° of each group In the case of Nb ΔH° has a large negative value, i.e., the solution of nitrogen is exothermic So, if the shallow potential minimum of weak adsorption is neglected, the apparent activation energies for nitrogen absorption(Q_{ab}) and desorption(Q_{des}) are related to that for elementary steps and the heat of solution(ΔH°) as follows

$$Q_{ab} = Q_{diss} \tag{2.53}$$

and

$$Q_{des} = |\Delta H^{\circ}| + Q_{ab} \tag{2.54}$$

With these energetic relationships it can be predicted easily that desorption rate is slower than absorption rate in the system with exothermic solution reaction if the driving force, i.e., concentration differences between the initial and the final state is identical In contrast, when ΔH° is positive such as for Mo and W, i.e., the solution reaction is endothermic, those are

$$Q_{ab} = 1/2\ \Delta H^{\circ} + Q_{tr} \tag{2.55}$$

and

$$Q_{des} = Q_{tr} \tag{2.56}$$

with Q_i assumed to be equal to Q_{tr}. In the previous equations, ΔH° refers to the value for one mole of A_2 and thus numerical values are twice the values given in unit of cal/g-atoms. Based upon the same reasoning as for exothermic reaction desorption rate is faster than absorption rate in endothermic solution reaction.

Kinetic Models on High Temperature Gas/Metal Reactions

A variety of kinetic aspects of high temperature gas/metal reactions has led to development of many kinetic models including the different reaction mechanisms and rate laws. Most of gas/metal reactions, however, can be accomplished through three basic steps any one of which may dominate or influence the overall reaction rate. These are:

i) gas phase transport in which reactant species move between the gas and the interface

ii) interface reaction which occurs at the interface with adsorption or desorption occurring as necessary

iii) liquid phase transport in which reactant species move between the interface and the interior of metal

Hence, step(i) and step(iii) are physical in character while step(ii) is chemical. The composition profiles in the gas phase and metal are shown schematically in Fig. 2.17 for each type of reaction control.

In the sections to follow, the kinetic aspect of each step will be discussed with specific experimental results associated with gas-Nb reactions together with gas-other refractory metals.

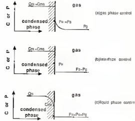

Cm the mean concentration of the dissolved substance in the liquid
Cms- the concentration of the dissolved substance at the surface
Pe the equilibrium pressure corresponding to Cms
Ps the pressure at the surface
Pg the mean pressure in the gas phase

Fig 2.17 Concentration and partial pressure profile for different types of rate control in degassing process

Mass Transfer in the Gas Phase

When species A in a gas stream of A + B mixture is under the influence of concentration gradient, the molar flux of A relative to stationary coordinate is made up of two parts: $-CD_{AB}\nabla X_A$ which is the diffusion contribution and $X_A(N_A + N_B)$ which is the molar flux resulting from the bulk motion

$$N_A = CD_{AB}\nabla X_A + X_A(N_A + N_B) \tag{2.57}$$

where N_A and N_B are molar fluxes of A and B, C is the concentration of A + B, D_{AB} is the diffusivity of A in A + B mixture, and X_A is the molar fraction of A. If bulk motion resulting from volume change caused by surface chemical reaction does not exist, the second term in equation (2.57) can be neglected. Dissolution reaction of diatomic gases like N_2 or H_2 belongs to this category. Then mass transfer in the gas boundary layer can be described as follows

$$N_A = -CD_{AB}\nabla X_A \tag{2.58}$$

Assuming that the A + B gas mixture behaves ideally, integration of equation (2.58) over the boundary layer, δ, gives

$$N_A = \frac{P}{RT_f}\,\frac{D_{AB}}{\delta}\,(X_A^b - X_A^i) \tag{2.59}$$

where b and I refer to the bulk and interface, respectively, and T_f is equal to $1/2(T_b + T_i)$. This equation can be rewritten in terms of wt%/dt and partial pressures as

$$dC_A/dt = -\frac{100M_A A}{WRT_f}\,\frac{D_{AB}}{\delta}\,(P_A^b - P_A^i) \tag{2.60}$$

where C_A is the concentration of A in the gas in wt%, M_A is the atomic weight of A, A is the surface area, W is the weight of the sample and P_A is the partial pressure of A. Since $C_A^2 = KP_{A_2}$, equation (2.60) yields

$$dC_A/dt = \frac{100M_AA}{WRT_f} \frac{D_{AB}}{\delta} \frac{1}{K} (C_A^2 - C_A^2) \tag{2.61}$$

This equation implies that if gas phase transport is rate controlling in diatomic gas dissolution reaction, then the reaction should be second order with respect to C_A

On the other hand, the molecular flux due to bulk motion should be taken into account if the surface reaction results in volume change. For example, consider the decarburization by oxygen, $C_{in\ metal} + O_2 = 2\ CO$ In this reaction, the net flux of gas takes place away from the metal since two moles of CO gas are generated for each O_2 molecule reacting with the metal Thus, the net flux away from the metal should decrease the rate of transport of reacting species. In such case equation (2.57) can be applied without neglecting the second term.

$$N_{O_2} = -CD_{O_2-CO}dX_{O_2}/dx + X_{O_2}(N_{O_2} + N_{CO}) \tag{2.62}$$

where C is the concentration of O_2 + CO D_{O_2-CO} is the diffusivity of O_2 in O_2 + CO mixture, and X_{O_2} is the molar fraction of O_2. N_{O_2} and N_{CO} are molar fluxes of O_2 and CO, respectively. Plugging $N_{CO} = -2N_{O_2}$ in integrating the equation (2.62) over the gas boundary layer, δ, it gives

$$N_{O_2} = \frac{P}{RT_f} \frac{D_{O_2-CO}}{\delta} \ln \frac{1+P_{O_2}^b/P}{1+P_{O_2}^s/P} \tag{2.63}$$

where P_{O_2} is the partial pressure of oxygen Using $\ln(1+P_{O_2}/P) = P_{O_2}$ when P_{O_2} is small compared with total pressure of 1 atm, equation (2.63) can be reduced to

$$N_{O_2} = \frac{P}{RT_f} \frac{D_{O_2-CO}}{\delta} (P_{O_2}^b - P_{O_2}^s) \tag{2.64a}$$

or

$$dC_O/dt = -\frac{100M_{O}A}{WRT_1}\frac{D_{AB}}{\delta}\frac{1}{K}(C_{s}^{2} - C_O^{2}) \qquad (2.64b)$$

Again, this equation indicates that the reaction is a second order if gas phase transport is rate controlling in case the surface reaction causes volume change

On the other hand, close examination of equations(2.61) or (2.64b) indicates that only D_{AB} and δ are unknown parameters. An estimation of gas phase mass transfer coefficient, k_G, which is defined as D_{AB}/δ, can be made from the Steinberger and Treybal equation [60Ste], which relates the Sherwood number to other dimensionless groups associated with a variety of variables controlling the systems. Their equation is

$$Sh = 2 + 0.5\,(Gr\,Sc)^{0.25} + 0.35(ReSc^{0.5})^{0.62} \qquad (2.65)$$

and Gr' in the above equation is defined as

$$Gr' = GrM + (Sc/Pr)^{0.5}\,GrH \qquad (2.66)$$

where each notation indicates the followings

Sh, Sherwood number, $(= k_G d/\bar{D})$

GrM, Grashof number for mass transfer $(=gd^3\rho_f(\rho_i-\rho_b)/\mu_f^2)$

GrH, Grashof number for heat transfer $(=gd^3\rho_f(T_i-T_b)/\mu_f^2T_f)$

Pr, Prandtl number $(=\mu C_p/k)$,

Re, Sphere Reynolds number $(=\rho_f dV/\mu_f)$

Sc, Schmidt number $(=\mu/\rho\bar{D})$,

k_G, gas phase mass transfer coefficient (cm s^{-1})

d, diameter of specimen (cm)

$\bar{D}$, interdiffusivity (cm^2 s^{-1})

ρ; density (g cm^{-3})

μ, viscosity of gas (g cm^{-1} s^{-1})

T; temperature (K)

V, velocity of gas (cm s^{-1})

C_p, heat capacity of gas (J g^{-1} K^{-1})

k thermal conductivity of gas (J cm^{-1} s^{-1} K^{-1})

g, acceleration due to gravity (cm s^{-2})

i, interface

b bulk

f film

The equation(2.65) involves the linear addition of the respective contributions due to radial diffusion such as would occur in a static isothermal system(1st term), free convection which would arise with a liquid metal droplet which is hotter or colder than the gas even without any imposed gas flow(2nd term), and forced convection which arises from the gas flow under isothermal conditions(3rd term). At low temperatures the first and the third terms are the most important but at high temperatures, all three terms are equally important. If the absorption or desorption processes proceed with all parameters except the gas flow rate fixed, the first and second terms in equation (2.65) will remain constant. Only the third term will be affected by gas flow velocity because Reynolds number includes the gas velocity term. This, in turn, will affect the mass transfer coefficient, k_g, which is included in the Sherwood number. This idea is often used in determining whether or not gas phase transport is the rate controlling step. Validity of equation(2.65) has been tested by a number of high temperature experiments[67Bak, 71Fru, 85Lee, 85Rao, 86Bat]. For example, in the deoxidation study of copper by 1% hydrogen in nitrogen[71Ric] it has been found that at temperatures between 1400 and 1600 °C the values of k_g derived from the experiments agree well with the values derived from the equation(2.65). Good agreement between the experimental and calculated values for various flow rates is also reported in the copper oxidation at 1600 °C under the nitrogen atmosphere containing a small amount of oxygen [70Gle ,71Ric].

Therefore, in the light of all the above discussion it can be summarized that if gas phase transport is the rate controlling step, then

(1) absorption (or desorption) rate would be proportional to $(P_A^b \quad P_A^i)$, or $(C_A^{b2}-C_A^{i2})$ in the dissolution reaction of diatomic gas, i.e., second order with respect to $[C_A]$

(2) gas/metal reactions can be assumed to be controlled by transport in the gas phase when the rate is markedly influenced by gas velocity because k_g is related to Reynolds number which includes the gas velocity term.

Transport in Liquid Phase

The mass transport in the interior of the liquid phase is affected by convection, which may be generated by artificial means such as induction stirring or blowing gases through the melt. It may also be induced spontaneously by differences in the density of the melt between the surface and the interior, which is caused by temperature difference resulting from heat loss from the surface of the melt. The convection can accelerate equalization of the concentration within the melt. But it is to be realized that the most important process in liquid phase transport is the transport to the gas/liquid phase boundary, taking place by diffusion in the liquid boundary layer

The boundary layer mass transport rate is proportional to the concentration difference between the interior and the surface of the melt. The rate is therefore

$$dC_m/dt = \beta(A/V)(C_m - C_{ms}) \qquad (2.67)$$

where C_m is the concentration in the interior of the melt and C_{ms} is the concentration at the surface which is in equilibrium with the partial pressure of the substance to be removed outside the melt, and β is the mass transfer coefficient in liquid which has the dimension of Cm/sec. In a similar manner to that in gas phase transport, β is related to diffusion in the boundary layer as

$$\beta = D/\delta \qquad (2.68)$$

where D is the diffusivity of element of concern in the melt and δ is the thickness of boundary layer. Thus it can be seen that the mass transfer coefficient depends mainly upon diffusivity of a component of interest in the liquid and hydrodynamic factors affecting the thickness of boundary layer. In contrast to gas phase transport, there is no reliable means to estimate the mass transfer coefficient for the interior of the liquid metal because of the poor knowledge of liquid flow during electromagnetic levitation. However, it is well known that a great deal of movement goes on in both the surface and the interior of the levitated droplet although this movement varies to a great extent with the metal and with the size of liquid droplet. Two gram drops of iron, for example, have been observed to pulsate at the frequency of about 40 Hz with the diameter changing each cycle by a factor of two.[71Ric]

Some experimental results make it certain that such movement enhances the mass transfer in the liquid metal. In the experiment on deoxidation of the levitated copper droplet in hydrogen and oxidation of nickel in oxygen[71Rao], the mass transfer coefficient of 0.2 Cm/sec was obtained. This value permits an 8 mm diameter drop weighing about 2 gram to come halfway to equilibrium concentration in 0.46 second. In comparison, a rigid drop of similar size would bring its average concentration halfway to equilibrium in 48 sec for a diffusion coefficient of 10^{-4} Cm^2/sec. The diffusion coefficients of oxygen in copper at 1100 °C and in iron at 1550 °C are $4\cdot10^{-5}$ and $8\cdot10^{-5}$ Cm^2/sec, respectively. Thus it can be seen that fluid motion in the levitated drops enhances material transport to surroundings 100 times faster than the droplet without motion. Another interesting results of the mass transfer in levitated melt is shown in Lee and Rao's experiments[82Lee] in which the effective diffusivity of carbon in an iron-carbon droplet levitated in the electromagnetic field was about 10 times as large as that in the similar melt contained in the crucible. This also indicates that a vigorous motion present in the levitated droplet enhances the mass transfer in the liquid phase to a great extent.

In summary, if liquid phase mass transport is rate controlling, the overall reaction will be

(1) first order with respect to $[C_A]$ in the solution reaction of diatomic gases

(2) affected by the change in hydrodynamic condition of levitated droplet

However, the liquid phase transport is rarely found to be a rate controlling step in the gas - levitated liquid metal reaction under electromagnetic field because of great enhancement of mass transfer due to vigorous stirring

Interface Chemical Reaction

In dealing with the kinetics of the gas/metal reactions, interfacial chemical reactions again can be divided into some substeps When the forward and the backward reactions in this stage are accomplished through the same substeps but in reverse sequence, it is called a reversible reaction. On the contrary, in some cases, the forward and backward reactions undergo the different reaction routes. This type of reaction is a irreversible reaction.

Reversible reaction

Under certain conditions of pressure and temperature, the reactions of metals with diatomic gases such as H_2, N_2, and O_2 leads to a solution reaction which can be represented as

$$A_2(g) \quad = \quad 2A(diss) \tag{2.69}$$

For some metal-gas systems the range of gas pressure in which this equilibrium is established is extremely low since, at high pressures, compounds such as nitrides and oxides, are formed. However, in systems like Fe-N, Ta-N, and Nb-N, the reaction(2.69) can easily be stated over a wide range of pressures Considering the absorption of the gas A_2 in metal the following partial steps can be distinguished in the interfacial chemical reaction (a) adsorption of gas molecule on the metal surface (physical adsorption), (b) dissociation of the gas molecules and strong adsorption of the atoms (chemisorption) and (c) transfer of the gas atoms through the metal surface

$$
\begin{aligned}
A_2(g) &= A_2(ad) \\
A_2(ad) &= 2\ A(ad) \\
A(ad) &= A(diss)
\end{aligned}
\tag{2.70}
$$

In desorption, the same steps occur in the reverse sequence. In the section to follow, experimental results supporting each elementary step will be discussed.

Dissociative chemisorption Horz and Steinheil[71Hor1, 71Hor2], Feng[70Fen] and Rosner and et al[73Ros, 75Ros] have studied the nitrogen absorption in solid Ta and Nb(thin specimen with thickness less than 0.5 mm, where diffusion plays no important role) at temperatures above 1000 °C in pressures ranging from 10^{-6} to 10^{-3} Torr. The initial absorption rate v_o was found to be proportional to the nitrogen pressure and dependent on reaction temperature with an activation energy of about 67 kJ/ mole N_2. The rate equation was given as

$$r = k\ P_{N_2} - k'C_N^2 = k\ P_{N_2}(\ 1 - C_N^2/C_{Ne}^2) \tag{2.71}$$

where k and k' are the rate constants for the forward and backward reactions, respectively and C_{Ne} denotes the equilibrium value of the nitrogen concentration in the metal. These results show that the absorption of nitrogen by Ta and Nb specimens is controlled by the dissociative chemisorption of nitrogen.

The kinetics of nitrogen desorption from Nb were investigated in high vacuum for thin specimen(δ < 0.5 mm) at temperatures between 1700 - 2200 °C and initial concentration C_o less than 6.5 at % N [75Ros, 75Fen, 66Geb]. A second order rate law is reported with high activation energies of about 519 kJ/mole N_2

indicating that recombination of nitrogen atoms to molecules is the rate controlling step.

However, Rosner and Coworkers[75Ros] found that dissociation and recombination are rate controlling for nitrogen absorption and desorption of Ta only in a definite range of lower temperatures and low pressures while at high temperatures and pressures, either the transfer of atoms through the surface or bulk diffusion becomes rate controlling.

Transfer of atoms through the metal surface Jehn[70Jeh], Fromm[71Fro1], and Evans[69Eva] investigated the nitrogen desorption in Mo-N and W-N systems. It was reported that desorption of molecular nitrogen began at a temperature of about 1200 °C and the rate laws were of the first order, i.e., $v = -k\,C_N$, with relatively small activation energy of about 92 kJ/mole N. Their analysis of the kinetic data indicated that at the onset of the reaction, transfer of atoms from the dissolved to the chemisorbed state is the rate controlling step whereas for longer reaction times diffusion of the nitrogen atoms to the metal surface should be the rate determining step even with the thin specimens. It may be concluded from the nitrogen desorption studies that the nitrogen absorption in Mo and W is proportional to $(P_{N_2})^{1/2}$ with higher activation energies than found for the Vb metals. The rate law for the net reaction

$$v = k\,(P_{N_2})^{1/2} - k\,C_N = k\,(P_{N_2})^{1/2}(1 - C_N/C_{Ne}) \tag{2.72}$$

is attributed to the rate control by the transfer of nitrogen atoms through the metal surface.

The differences in the kinetics and the activation energies of nitrogen absorption and desorption for Ta and Nb on the one side and Mo and W on the other side can be correlated with the enthalpies of nitrogen solution since the dissolution of nitrogen is highly exothermic for Nb and Ta whereas highly endothermic for Mo and W.

Irreversible reaction

In contrast to the metal - hydrogen or nitrogen systems, absorption and desorption of oxygen in many metals are irreversible. While oxygen absorption reaction passes through the same sequence of reaction steps as discussed for reversible reactions earlier, oxygen desorption is done by the formation of a metal oxide on the metal surface and the subsequent evaporation of this oxide into the gas phase. In general, several oxides may form and evaporate simultaneously. In a vacuum chamber these oxides condense on the wall, resulting in their removal from the reaction system. Considering only the evaporation of one oxide MeO, the mechanism of irreversible absorption and desorption of oxygen can be described by the following reaction sequences.

$$
\begin{aligned}
&\text{(a) } O_2(g) = O_2(ad) \\
&\text{(b) } O_2(ad) > 2\,O(ad) \qquad (2.73) \\
&\text{(c) } O(ad) + Me > MeO(g) \\
&\text{(d) } O(ad) = O(diss)
\end{aligned}
$$

In the following, kinetic studies related to Nb-O system will be dealt together with other refractory metal/oxygen systems exhibiting the similar behaviors

At temperatures below 1400 - 1600 °C and pressures below 10^{-3} Torr O_2, the reaction of Vb metals, Nb, and Ta, with oxygen results in the solution of oxygen in the metals. Under these conditions, and using thin specimens, the kinetics of absorption of oxygen by Vb metals have been investigated by many researchers [68Hor1, 72Hor1, 76Hor1, 75Fen, 76Jeh, 65Pas, 65Kof, 88Sch, 77Gra]. For sufficiently short reaction times, the oxygen absorption was reported to be described by the following rate law[68Hor1, 72Fro1]

$$v = \frac{k_a P_{O_2}}{1 + k_b \exp(Q/RT)} \tag{2.74}$$

The rate constant k_a and k_b can be attributed to steps a and b in the reaction scheme described in equation (2.73). The activation energy of oxygen absorption is Q = 47.3 kJ/moleO_2 for V, 59.6 kJ/moleO_2 for Nb and 73.7 kJ/moleO_2 for Ta. Values of oxygen absorption rate, v, decreases in the sequence V, Nb, and Ta. The rate equation(2.74) implies that both the transport of the gas molecules to the metal surface and the dissociative chemisorption of the gas molecules are rate determining.

The kinetics of oxygen desorption by the evaporation of oxides in high vacuum have been investigated in thin specimens of Nb at temperatures above 1400 °C[64Geb, 65Pas, 73Hor]. Desorption begins at temperature of 1600 °C for Nb with the formation of volatile oxides, NbO and NbO_2. At oxygen concentrations of less than 1 at%O, the evaporation of NbO predominates while at high oxygen concentrations the evaporation rates of NbO and NbO_2 are comparable, leading to the rate law as

$$v = k_1 C_o + k_2 C_o^2 \tag{2.75}$$

where k_1 and k_2 are rate constants for NbO and NbO_2 evaporations, respectively, and C_o is the oxygen concentration in Nb. Rosner and Co-worker[75Ros, 76Ros] studied simultaneous oxygen absorption and desorption due to suboxide evaporation in the Ta-O system at temperatures between 2100 and 2500 °C and pressures between $1.2 \cdot 10^{4}$ and $5 \cdot 10^{5}$ atmosphere. Based upon experimental data it was demonstrated that the mechanism shifts from adsorption control at lower oxygen pressures and temperatures to the interface penetration control at higher oxygen pressures and temperature [76Ros]. With the aid of energy diagrams similar to Fig. 2.16, it can be speculated why oxygen is not desorbed as an oxygen molecule in the oxygen group Vb metal systems while nitrogen is desorbed as a nitrogen molecule. In solid niobium, solution enthalpy of nitrogen is − 177.82 kJ/g atom N and that of oxygen is − 386.18 kJ/g atom O. This indicates that oxygen dissolution is also exothermic reaction but with much higher ΔH°. Accordingly, comparing the energetic conditions for a molecular desorption of oxygen with that for the desorption via the evaporation of oxides it can be surmised based upon the observed experimental results that the oxide evaporation is energetically more favorable than the molecular desorption as far as oxygen escape is concerned.

On the other hand, when oxygen absorption in Nb or Ta occurs without simultaneous oxide evaporation at low temperatures, a small degree of surface coverage $\theta \ll 1$ can be assumed only for short reaction times. As the absorption proceeds and in turn, increases oxygen concentration in the bulk metal, the surface coverage of oxygen keeps increasing, resulting in the decrease of oxygen absorption rate. G. Horz and et al[70Hor, 68Hor1, 68Hor2] found in Nb-oxygen system that the reaction coefficient, r, which is the fraction of the amount of oxygen dissolved in Nb among the oxygens delivered from the bulk gas to the interface, is related to the surface coverage by the following expression.

$$r = \frac{\alpha}{1 + k_s^* \exp(Q/RT)/(1-\theta)^2} \tag{2.76}$$

where α is a constant near unity. From equation (2.76), the data on the surface segregation of oxygen on the Nb surface can be obtained because the initial value of r_o is available for short reaction times with $\theta \ll 1$[77Gru, 77Kla]. Such an evaluation of the kinetic data is based on the facts that, during oxygen absorption, quasi-equilibrium between the dissolved and the adsorbed is established. For the Nb-O system, the value of segregation enthalpy was obtained to be - 50 to - 63 kJ/mole O [77Gru, 77Kla].

The reaction coefficients for nitrogen – metal and oxygen – metal systems are plotted logarithmatically as a function of 1/T in Fig. 2.18. It can be seen that in the oxygen systems the values of reaction coefficient becomes smaller in the sequence V, Nb, and Ta. The reaction coefficient is much larger in the oxygen niobium system than in the nitrogen niobium system, indicating that niobium-oxygen solution reaction takes place much faster than niobium-nitrogen reaction.

Reactions under Dissociation and Formation of Carbon Monoxide

K. Ono and et al. [80Ono] investigated the deoxidation and decarburization of Nb through CO evolution for the samples containing various combination of C and O contents at temperatures between 2073 and 2473 K and at the CO partial pressure of $1.3 \cdot 10^{-2}$ Pa. Their results showing the carbon and oxygen contents before

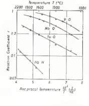

Fig. 2.18 Reaction coefficients for the absorption of oxygen or nitrogen in the system V-O, Nb-O or Ta-O, or Nb-N as a function of the reciprocal absolute temperature(thin samples, solid solution range low gas partial pressures, sufficiently short reaction times) [72Hor1]

and after vacuum degassing are plotted in Fig. 2.19. Based on the experimental results, they concluded that

(1) If an excess of carbon is present in Nb before degassing, carbon and oxygen can be removed by the C/O atomic ratio equal to 1 and carbon remains after degassing.

(2) On the other hand, if oxygen is present in excess, degassing proceeds with atomic ratio of C/O smaller than unity and the carbon can be effectively removed at the same time.

(3) Oxygen impurity can be eliminated even if the carbon is not present.

A similar behavior was also obtained in degassing of liquid Nb containing both C and O as seen in Fig. 2.20. Based on the above results, it may be surmised that degassing in Nb containing carbon impurity proceeds by the decarburization through CO evolution or deoxidation via suboxides evaporation together with CO evolution depending on the ratio of C/O. For effective purification of Nb containing both oxygen and carbon, the metal should contains oxygen in excess initially.

Decarburization of Nb containing carbon in excess can be attained by annealing this metal in an oxygen stream to form carbon monoxide according to

$$2\ C(diss) + O_2(g) \quad > \quad 2\ CO(g) \tag{2.77}$$

At the same time, solution of oxygen in the metal may occur

$$O_2(g) \quad > \quad 2\ O(diss) \tag{2.78}$$

The decarburization kinetics of Nb containing from 0.3 to 1 at % C have been investigated for thin specimens at temperatures between 1600 and 2120 °C and oxygen partial pressures between $2 \cdot 10^{6}$ and $5 \cdot 10^{3}$ torr[72Hor1, 72Hor4, 73Hor2]

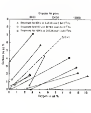

Fig. 2.19 Correlation of the carbon and oxygen levels in niobium before and after the vacuum degassing in solid state.[80Ono]

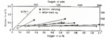

Fig. 2.20 Correlation of the carbon and oxygen levels in niobium before and after melting in the electron beam furnace for 600 seconds [80Oao]

Analysis of the kinetic data supports a reaction mechanism as presented schematically shown in Fig. 2.21 Characteristic for these reaction mechanisms are that the dissociative chemisorption of oxygen, step II is not reversible and that the oxygen chemisorbed at the metal surface can dissolve in the metal(step III) or can react with chemisorbed carbon to form carbon monoxide(step V). Thus steps III and V are competing reactions. Two reaction ranges exist in the case of the decarburization of Nb. At short reaction times, excess carbon is present at the surface and all the chemisorbed oxygen reacts with carbon to form carbon monoxide without oxygen dissolution in the metal In this case, decarburization is controlled by the transport and dissociative chemisorption of oxygen At longer reaction times oxygen is present at the surface in excess and dissolve partially in the metal. In this regime, for the formation of carbon monoxide the delivery of carbon from the metal bulk to the surface is essential and is found to determine the overall reaction rate.

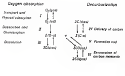

Fig 2.21 Reaction scheme for the decarburization of Vb metals in flowing oxygen.[72Hor]

CHAPTER 3.
EXPERIMENTAL

All experiments in this study were performed by electromagnetic levitation technique. This technique is particularly suitable for studying gas-Nb melt interactions because niobium with high melting point and its reactive characteristics can be melted without contact with a crucible, preventing contamination by crucible materials. In the section to follow, the principles of this technique will be discussed in detail.

Electromagnetic Levitation Technique

When a conductor is placed in an alternative magnetic field, it experiences heating and force due to the induction of eddy currents inside it. Sample heating results from eddy current loss while force arises from Lorentz magnetic forces due to the interaction between eddy currents in the sample and applied currents in the coil. This force acts in such a direction so as to have the conductor move from a stronger to a weaker part of the magnetic field. So, when a metal is heated in two coaxial coil with conical shape as shown in Fig. 3.1, a levitation force is generated by the field strength of bottom coil decreasing in the upward vertical direction [65Fro3, 65Pei, 71Boe, 84Erh]. At the same time, a lateral stability results from the field strength which decreases radially toward the field axis and, in turn, produces a

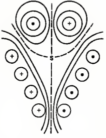

Fig 3 1 Schematic diagram of levitation coil restoring force toward the center of the coil. The upper oppositely wound coil together with a gravitational force keeps the sample forced down into the bottom coil, making the sample heated with efficiency and stability.

Electromagnetic levitation technique has the following advantages for studying gas-metal reaction at high temperature [60Beg, 65Fro1]

1) The specimen is melted while suspended in the space thus eliminating contamination from a crucible or container
2) Good homogeneity is achieved in the melt because of the vigorous stirring action of the electromagnetic fields
3) No considerable temperature difference exist in the specimen
4) Melting is generally very rapid, often occurring in less than a minute

Materials

Niobium used in this study was obtained from Cabot Corporation in the form of rod with 0.635 Cm diameter. The composition analysis is given in Table 7. Niobium rods were sheared into cylindrical pieces weighing 2.1 ± 0.1 gram. Close control of specimen weight ensured that the nearly same surface area existed in all the experiments. The surface of each specimen was cleaned with acetone to remove contaminants like grease and oil which ought be introduced inadvertently during weighing and handling.

The purities of gases used in this investigation are shown in Table 8. All gases were dried by passing them through drierite columns. Trace amounts of oxygen in the inert gases were eliminated by passage through a column filled with

Table 7 Chemical analysis of Nb, ppm

Element	N	O	C	H	Ta	Al	Si	Fe	Nb
Concentration	15-30	85-125	15-25	5-10	395-790	10-15	0-10	10-25	Bal

Table 8 Composition analysis of gases

	purity	impurities(ppm)							
		Ar	He	Ne	O_2	CO_2	H_2O	N_2	THC*
Ar	99.996%		10	8	1	0.5	5	5	0.5
He	99.995%	5		5	3	2.0	8	20	0.5
N_2	99.995%	25	2	8	3	2.0	5	-	0.2
CO	99.99 %		3		10	15	5	50	10

* THC indicates total hydrocarbon.

titanium sponge held at 800 °C. The CO_2 impurity present in CO gas was removed by passing the gases through ascarite columns.

Apparatus

Fig. 3.2 shows the details of the experimental set-up used in this study. The power source for levitation was Lepel 10 kW R.F. generator. It was normally operated at 25 - 60 percent of its maximum power. The levitation coil was formed from 1/8 " O.D., thin walled copper tubing wrapped with glass fiber tape for insulation. It had a conical shape with 16 mm I.D. at the bottom and the full conical angle of 30 degree. The coil had 14 turns, the top one opposite in direction to the lower 13 turns among which the outside 6 turns are wound on the inside 7 turns in the same direction. The reaction chamber consists of a 5/8 " O.D. glass tube open at both ends and connected to a gas delivery system.

Temperature was measured by a single color pyrometer calibrated against the melting temperature of pure Nb. The error in temperature reading was ± 10 °C. Some degree of temperature control can be obtained by adjusting the output power level. In order to increase the heating effects thereby increasing the sample temperature, the power must be lowered to have the sample rest lower in the bottom coil in order for more dense magnetic flux to go through the sample.

The gas flow was measured using calibrated spherical float flowmeters within the accuracy of 2%. The gas mixture with a desired partial pressure of N_2 or CO was prepared by adjusting the flow rates of N_2 or CO and Ar gases at room temperature using the regulating valves of the flowmeters. The rapid switch of gas atmosphere from the inert to the reactive or vice versa, which is essential for

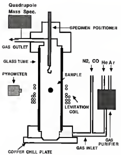

Fig. 3.2 Schematic diagram of experimental set-up.

the prevention of time delay of the reaction start, was done by placing a four way stop cock near the gas inlet to levitation column.

Procedures

At the beginning of each run, a specimen is lowered to the levitation position by a specimen positioner. A flow of Ar and He gases then was maintained through the reaction column for approximately 30 seconds. After the reaction column was purged by inert gas mixture, the power was turned on, levitating the specimen. At that time, the specimen positioner was raised up to prevent contact with the sample during melting. Then a He flow keeps decreasing slowly in order to increase the temperature of specimen up to melting point of niobium. After about 5 7 seconds arrest at melting temperature, the sample temperature keeps increasing and, finally, is stabilized at a certain level which depends upon the levitation position of sample in the coil. At this point, reaction temperature could be adjusted to the desired temperature by controlling the power, thereby controlling the levitation position. Once sample temperature reached a desired level, the argon gas was replaced with a N_2 + Ar gas mixture with a predetermined mixing ratio almost instantaneously. This was taken as time zero for measuring the reaction time. After reacting the sample with nitrogen in levitated state for a desired length of time, the sample was dropped and quenched on a copper chill plate by cutting off the power to the levitation coil. Simultaneously, the flow of Ar + N_2 gas was replaced with a Ar + He flow. The total flow rate was maintained constant all the time. This ensured to minimize the change in flow pattern in the gas phases when nitrogen gas was introduced.

The partial pressure of nitrogen gas varied depending upon the experimental conditions. For the study of nitrogen absorption, the desired nitrogen partial pressure was obtained by adjusting the flow rates of N_2 and Ar gases. However, in studying the effect of gas flow rate on the absorption behavior, a Ar + 5.14 %N_2 gas mixture premixed in the factory was used to prevent the possible small fluctuation of partial pressure in each run. Using the procedure described above, the absorption behavior of nitrogen in liquid Nb was investigated under various conditions of total gas flow rate, partial pressure, temperature, and time.

In studying the desorption behavior of nitrogen in liquid Nb, the specimen was initially saturated with nitrogen by exposing it to N_2 + Ar mixture with nitrogen partial pressure of 0.15 atm for 4 minutes, which was found to be long enough to saturate nitrogen in most of absorption conditions from the absorption experiments. The gas atmosphere was then changed to a pure Ar or Ar+N_2 gas mixture with lower partial pressures of nitrogen instantaneously. Through such procedures, the desorption kinetics were studied as a function of partial pressure, and processing time.

The carbon and oxygen absorption/desorption experiments were carried out in a flow of CO + Ar gas mixture with various partial pressures of CO. In the study on the effect of gas flow rate, Ar + 3% CO premixed gas was used. Most of experimental procedures was basically the same as those in nitrogen experiments. The carbon and oxygen absorption kinetics were examined as a function of gas flow rate, CO partial pressure, temperature and reaction time In desorption studies, initially carbon and oxygen were absorbed in the sample in the CO + Ar atmosphere with CO partial pressure of 0.03 atm. at 2813 K for 4 minutes This treatment time was found to be adequate for producing saturated C and O samples Then the gas atmosphere was changed into desorption atmosphere of Ar or Ar + CO with lower partial pressure of CO.

The composition analysis of the processed samples was conducted by two methods Nitrogen analysis was done (1)by measuring the weight gain/loss using the balance with the precision of 0.001 gram, and (2) by a flame atomic absorption method. Two methods gave essentially the same results except at the concentration higher than about 3.5 wt% Since the composition data measured by the flame atomic absorption method showed a scattering behavior for the duplicate samples in high concentration range, the % weight gain/loss data have been used to analyze the nitrogen absorption and desorption data It is to be pointed that since the vapor pressure of Nb at its melting point is = 10^{3} Torr[80Oha] the weight loss due to vaporization for 4 minutes(which is the longest processing time in absorption condition) under the experimental conditions used is estimated to be about $4 \cdot 10^{5}$ gram, which is negligible amount compared with the total change in weight. Therefore, the entire weight gain/loss could be attributed to nitrogen gained/lost.

On the other hand, carbon and oxygen contents of the samples were analyzed by the flame atomic absorption technique. The detectability limit of this technique was 0.0001 %

Quadrupole Mass Spectrometry

Change of partial pressures of reactant and product gases during the processing was monitored by a Quadrupole residual gas analyzer manufactured by AMETEK(model MA 200). Since the pressure of reaction column was estimated to be about 1 atmosphere, a pressure reduction system was attached to reduce the pressure to below 10^{-4} torr, allowable pressure range by a Quadupole analyzer, with a quartz capillary tube of 1 μm inside diameter. As soon as CO gas is introduced into the reaction column, monitoring of partial pressure is started by opening the valve to the analyzing chamber, which was already evacuated to ~10^{-6} Torr by turbomolecular pump. The precision of partial pressure reading is ±2 % according to the manufacturer's specification. Using these procedures, cracking patterns before and during the processing were obtained initially to identify which gases are involved in the reaction as reactant or product gases. In the next run, the change of partial pressures of gases of interest were monitored at a constant time interval to examine the kinetic characteristics of the reaction.

CHAPTER 4
EXPERIMENTAL RESULTS

Nitrogen

For the determination of solubility and the mechanism of nitrogen - liquid Nb interaction, experiments were performed to study the effects of partial pressure of nitrogen, temperature and time on the nitrogen absorption and desorption behavior. Prior to these experiments it was examined how gas flow rate affects absorption kinetics, providing the idea of the range of flow rate in which the effects of the above parameters can be studied independently of the gas flow rate. In the following section, the results will be dealt with in detail.

Effect of Gas Flow Rate on Nitrogen Absorption

The mass transfer rate in the gas boundary layer surrounding the melt is influenced by the flow rate of the gas stream as described in the previous chapter. In order to examine the effect of the gas flow rate on the nitrogen absorption kinetics, experiments were carried out at various flow rates of Ar + N_2 mixture ranging from 500 ml/min to 3800 ml/min, (60-456 in Reynolds number), all of which belong to laminar flow regime in the present experimental set-up. The nitrogen absorption data at the fixed processing times are plotted as a function of the gas flow rate in Fig. 4.1. In all cases, the nitrogen partial pressure and temperature were fixed at 0.0514 atm ($5.21 \cdot 10^3$ Pa) and at 2843 K. It can be seen that the amount of nitrogen absorbed increases with increasing the flow rate in

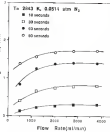

Fig 4 1 Nitrogen absorption behavior of liquid Nb as a function of gas flow rate lower flow regime at each fixed processing time. However, at the flow rates higher than 2000 ml/min, the change of nitrogen concentration becomes negligible with further increase of the gas flow rate. Such behavior supports the view that under the present experimental conditions the gas phase resistance to the overall nitrogen absorption process becomes insignificant at the flow rates higher than 2000 ml/min.

Effect of Temperature on Nitrogen Absorption

The effect of reaction temperature on absorption kinetics was investigated for three temperatures, 2743, 2843 and 2943 K. At each temperature, the absorption data were obtained for various lengths of time under a constant flow rate of 4000 ml/min of Ar + N_2 mixture but with different nitrogen partial pressures ranging from 0.0125 to 0.25 atm.($1.27 \cdot 10^3$ Pa to $2.54 \cdot 10^4$ Pa). Fig. 4.2 shows the variation of nitrogen concentration with time for different processing temperatures at fixed nitrogen partial pressures of 0.25, 0.15, and 0.05 atm. Nitrogen absorption is rapid at the initial stage but the rate decreases with increasing processing time as the sample becomes saturated gradually. The saturation time was around 4 minutes for most samples. The saturation concentration decreases with increasing processing temperature, indicating that the process of nitrogen absorption in liquid Nb is exothermic as will be discussed later. This finding is in good agreements with the observation that the sample temperature goes up sharply from the stabilized temperature above melting point at the instance the N_2 gas is introduced into the levitation chamber as shown in Fig. 4.3.

Effect of Nitrogen Partial Pressure on Nitrogen Absorption

In order to investigate the effect of nitrogen partial pressure, the data obtained at 2843 K under various partial pressures of N_2, namely, 0.0125, 0.05,

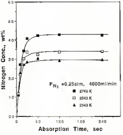

(a)

Fig. 4.2 Effect of temperature on nitrogen absorption in liquid Nb
(a) P_{N_2} = 0.25 atm (b) P_{N_2} = 0.15 atm (c) P_{N_2} = 0.05 atm

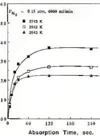
P_{N_2} = 0.15 atm, 4000 ml/min.
■ 2743 K
□ 2843 K
▲ 2943 K
Nitrogen Conc., wt%
6.0
5.0
4.0
3.0
2.0
1.0
0.0
0
60
120
180
240
300
Absorption Time, sec.

(b)

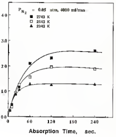
P_{N_2} = 0.05 atm, 4000 ml/min
■ 2743 K
□ 2843 K
▲ 2943 K
Nitrogen Conc., wt%
4.0
3.0
2.0
1.0
0.0
0
60
120
180
240
Absorption Time, sec.

(c)

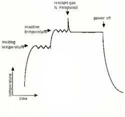

Fig 4 3 Typical temperature profile during nitrogen absorption

0.15, and 0.25 atm, are plotted against the processing time in Fig. 4.4. It can be seen that the increase in nitrogen partial pressure results in more rapid nitrogen absorption at the initial stage and a shorter time for nitrogen saturation. The saturation level, being dependent on the nitrogen partial pressure in the gas, increases as the partial pressure increases. Similar trends were also observed at two other processing temperatures, 2743 K and 2943 K.

Nitrogen Desorption

Fig. 4.5 shows the typical nitrogen desorption behavior for three nitrogen partial pressures at the reaction temperature of 2943 K. In this figure, the initial concentration is taken as the saturated concentration which is obtained by levitating the samples at 2843 K under the nitrogen partial pressure of 0.15 atm for 4 min. As discussed earlier, the gas flow was changed into pure Ar, 0.0125 atm N_2, or 0.05 atm N_2 atmospheres to make a desorption condition just after charging nitrogen in the sample. It is to be noted that the nitrogen desorbs rapidly at the initial stage and desorption rate levels off as degassing reaction goes on. The amount of nitrogen desorbed at a given processing time increases as nitrogen partial pressure in the gas stream decreases.

Carbon Monoxide

In order to determine the mechanism and the reaction rate of CO-molten Nb interactions, in addition to pressure-temperature-concentration relationship in the saturated state, the absorption/desorption behaviors of carbon and oxygen in CO atmosphere were studied under various combination of the processing variables, i.e.

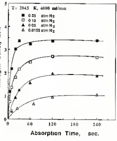

Fig. 4.4 Effect of nitrogen partial pressure on nitrogen absorption in liquid Nb

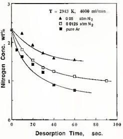

Fig. 4.5 Typical nitrogen desorption behavior in liquid Nb

partial pressure of CO, temperature, gas flow rate and the processing time. In the sections to follow, the effect of each parameter will be presented in detail.

Effect of CO Partial Pressure on C and O Absorption

The effect of CO partial pressure on absorption behaviors of carbon and oxygen in liquid Nb were studied in Ar + CO streams with different CO partial pressures. In this experiment, temperature and flow rate were fixed at 2813 K and 4000 ml/min. Absorption data for carbon and oxygen are shown as a function of processing time in Fig. 4.6 and Fig. 4.7, respectively. Data point corresponding to the same processing conditions in both figures are taken from the identical sample. It can be seen that carbon and oxygen are dissolved into liquid Nb together. This behavior indicates that the reaction, CO(g) = [C] + [O], plays an important role in the dissolution of C and O into Nb from CO gas. It can also be shown that carbon is saturated at a certain concentration depending upon the CO partial pressure. The saturation takes places at a higher concentration of C and in a shorter time as the partial pressure of CO increases. In all cases, the saturation time was less than 4 minutes. Similar behavior is also demonstrated for the oxygen absorption but the saturation level is lower compared with the C saturation concentration at a given CO partial pressure.

Effect of Temperature on C and O Absorption

Fig. 4.8 and Fig. 4.9 show the absorption behavior of carbon and oxygen at different reaction temperatures under CO partial pressure of 0.125 atm and flow rate of 4000 ml/min. At all reaction temperatures, liquid Nb is saturated with carbon and oxygen and saturation levels are lower with the increase of temperature. This trend

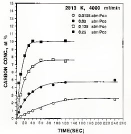

Fig 4·6 Effect of CO partial pressure on carbon absorption in liquid Nb

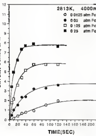

Fig. 4.7 Effect of CO partial pressure on oxygen absorption in liquid Nb

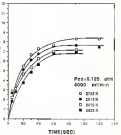

Fig. 4.8 Effect of temperature on carbon absorption from CO in liquid Nb

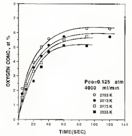

Fig. 4.9 Effect of temperature on oxygen absorption from CO in liquid Nb

indicates that CO dissolution reaction in liquid Nb is an exothermic process. In order to examine the interrelationship between carbon and oxygen concentrations during absorption, concentration data of the samples used in Fig.s 4.6-4.9 are plotted in Fig. 4.10. In this plot, C and O concentrations marked by each point were taken from the identical sample. It is of interest that there exists quite a good linear relationship between oxygen and carbon concentrations dissolved in liquid Nb indicating that $CO(g) = [C] + [O]$ plays a major role in the dissolution reaction. However, the constant atomic ratio of O/C of about 0.76 indicates that some other reaction takes place simultaneously as a side reaction, resulting in the oxygen loss or carbon surplus, as will be discussed later.

Effect of Gas Flow Rate on C and O Absorption

In order to check the effect of the gas flow rate on the absorption kinetics of CO in liquid Nb, the absorption behavior was studied by varying the gas flow rate in the range of 3000 to 6000 ml/min (360 to 720 in Reynolds number) with CO partial pressure and temperature fixed at 0.03 atm and 2813 K, respectively. Fig. 4.11 and Fig. 4.12 summarize the variation of C and O concentrations with the gas flow rate at fixed processing times. The amounts of C and O absorbed are affected slightly at lower flow rates in all cases but at the flow rates higher than 4000 ml/min, the changes of C and O concentrations become negligible with increasing the gas flow rate. Such behavior illustrates that the transfer rate of CO in the gas blanket is faster than the rates of other elementary steps at the flow rate at least higher than 4000 ml/min. Similar observation was made for N_2 - Nb absorption kinetics. Otherwise, absorption kinetics would have shown the dependence on the

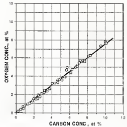

Fig. 4.10 Interrelationship between oxygen and carbon concentrations during CO absorption

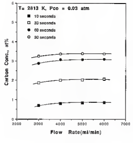

Fig. 4.11 Carbon absorption behavior of Nb from CO gas as a function of gas flow rate.

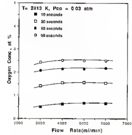

Fig. 4 12 Oxygen absorption behavior of Nb from CO gas as a function of gas flow rate gas flow rate since the thickness of boundary layer decreases with increasing the flow rate. Thus, it should be concluded that under the present experimental conditions the gas phase transport is not the rate controlling step.

Gas Phases Analysis by Quadrupole Mass Spectrometer

During the CO absorption, the partial pressures of CO and CO_2 of outlet gas were determined continuously using a quadrupole mass spectrometer. Fig. 4.13 shows the change of partial pressures of CO and CO_2 normalized against the input CO partial pressure with processing time. It can be seen that over the entire processing period CO_2 pressure remains nearly constant at about 5%, the value of which is the same as the CO_2 partial pressure of the residual gas in the analyzing chamber of Quadrupole mass spectrometer. On the other hand the initial CO pressure detected at the outlet is about half the input CO pressure at the onset of CO introduction into reaction section. As the reaction proceeds further, CO outlet pressure keeps increasing, finally reaching the state in which CO pressure remains nearly constant. Considering that the precision of pressure reading is ±2 % the discrepancy between the value of CO input and pressure reading at the final stage seems to come from the error of pressure readings or not long enough time for saturation. The observation described above indicates that initially about half of the CO input is removed from the gas phase as it dissolves in the liquid metal but the CO removal rate is decreased gradually as the process proceeds further, and it finally becomes negligible (the height of the hatched area is proportional to the rate of CO dissolution into the sample or the rate of CO removal from the gas phase). This behavior is in good agreement with initial rapid absorption of C or O in the

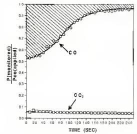

Fig. 4.13 Changes of partial pressures of CO and CO_2 of outlet gas during C and O absorption from CO gas.

interaction of CO with liquid Nb finally followed by the saturation to certain concentrations of C and O as shown in Fig 4.6 and Fig 4.7 Thus, it can be concluded from the present results that C and O absorption is accomplished through CO dissolution and exclude the possibility of the reaction, 2 CO = CO_2 + [C] in the absorption of C and O from CO gas.

C and O Desorption

Carbon and oxygen desorption behavior was studied in atmospheres of pure Ar and CO + Ar mixture with the CO partial pressure of 0.0075 atm, or 0.015 atm at 2813 K for the samples which were saturated with 0.03 atm CO gas at the same temperature. Concentration changes of carbon and oxygen during desorption are shown in Fig 4.14 and Fig 4.15 in which the concentrations at zero time correspond to the saturated ones at the processing conditions of CO charging prior to desorption experiment. There occurs a gradual decline in carbon or oxygen concentration but the rate slows down as time goes on It is also apparent that the carbon and oxygen desorb more rapidly with lowering CO partial pressure.

To examine the effect of temperature on the desorption behavior, the desorption experiments were carried out in a stream of pure Ar at 2753, 2813, 2873, and 2933 K for the samples saturated under the CO partial pressure of 0.03 atm at each temperature. Since the initial concentrations are different depending upon the saturation temperature, the raw concentration and the concentration normalized against the initial concentration are plotted together for carbon in Fig. 4.16 and for oxygen in Fig 4.17 Typical desorption behavior is observed at each temperature in that initial rapid desorption is followed by gradual decrease of desorption rate It is

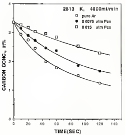

Fig 4 14 Effect of partial pressure of CO on carbon desorption in liquid Nb

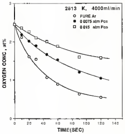

Fig 4.15 Effect of partial pressure of CO on oxygen desorption in liquid Nb

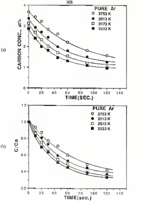

Fig. 4.16 Effect of temperature on carbon desorption in liquid Nb under pure Ar
(a) raw data (b)normalized concentration against initial concentration

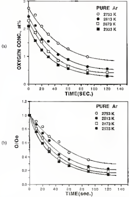

Fig. 4.17 Effect of temperature on oxygen desorption in liquid Nb under pure Ar
(a) raw data (b) normalized concentration against initial concentration

shown in the normalized concentration plots that the increase of temperature enhances the desorption rate over the entire period.

In Fig 4.18, the amount of oxygen desorbed is plotted against that of carbon desorbed in unit of atomic % for the samples used in Fig 4.16 and Fig 4.17 in order to reveal how one quantity is related to the other during desorption. In this graph, each point indicates one sample and each symbol represents the data obtained at the same temperature. The desorbed amount of each element is calculated by subtracting the values of concentration at each processing time from the initial concentration. The slope which is indicative of atomic ratio of oxygen to carbon in desorbed amounts, is approximately unity in all temperatures. This ratio implies that only the reaction [C] + [O] -> CO(g) is responsible for the observed desorption behavior, excluding the possibility of oxygen escape through the evaporation of niobium oxide in a pure Ar atmosphere. If both mechanisms were working together, the amount of oxygen desorbed would have been larger than that of carbon desorbed in a given desorption time, and would have shown a slope greater than unity. As described previously, the samples at the starting point of desorption contain carbon in excess since the initial concentrations of carbon and oxygen are the saturated values corresponding to CO dissolution condition. So, the present results agree well with the results reported by others[80Ono] in that only the desorption through CO evolution is responsible for C and O refining when the excess carbon exists in the sample. In this case, the excess amount of carbon will remain after oxygen is depleted.

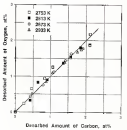

Fig. 4.18 Interrelationship between the desorbed amounts of oxygen and carbon in atomic % during CO desorption

CHAPTER 5
DISCUSSION

Nitrogen

From the thermodynamic calculations of the formation of Nb_2N presented earlier(see Table 4), it can be seen that the minimum nitrogen partial pressure for the formation of the compound is 0.3 atm. at 2773 K. Thus, excluded is the possibility of nitride formation on the surface of liquid Nb droplet under the experimental condition used in this study. Accordingly, only nitrogen solution reaction is taken into consideration in dealing with the solubility and the kinetic modelling.

Solubility of Nitrogen

The solution reaction of nitrogen in Nb may be described by the following equation

$$1/2\ N_2(g) = N\ (\text{in liquid Nb}) \tag{5.1}$$

the equilibrium constant, K, for the reaction is given by

$$K = \frac{a_N}{P_{N_2}^{1/2}} = \exp\left(\Delta G^\circ/RT \right) \tag{5.2}$$

where a_N is the activity of N in liquid Nb at temperature T, P_{N_2} is the partial pressure of nitrogen in the gas, and ΔG° is the Gibbs energy change for the solution reaction. As discussed earlier, if the solution obeys Henry's law and hypothetical 1 wt % solution of nitrogen is taken as the standard state, the activity term in

Equation (5.2) can be directly replaced by wt.% Consequently, Equation (5.2) becomes identical with Sieverts law, and the concentration of N in Nb can be related to the partial pressure of N_2 as follows

$$C_N = \exp\left(\frac{\Delta S^\circ}{R} - \frac{\Delta H^\circ}{RT}\right) \; P_{N_2}^{1/2} = k(T)\; P_{N_2}^{1/2} \tag{5.3}$$

where C_N is the concentration of nitrogen in liquid Nb in wt.%, k(T) is the temperature dependent Sieverts constant, and ΔH° and ΔS° are the standard enthalpy and entropy of solution, respectively

Based upon Equation(5.3), the saturated nitrogen concentration at each nitrogen partial pressure and reaction temperature is plotted against the square root of nitrogen partial pressure as shown in Fig. 5.1 A marked deviation from linearity is observed at high nitrogen concentrations, indicating that Sieverts law does not hold over the entire range of temperatures and partial pressures investigated. Nevertheless, Sieverts law can be applied at low nitrogen concentration (below approximately 2 wt.%) Taking Sieverts constant at each temperature, k, which is the slope of the linear portion of the plots in Fig 5.1, the values of log k are plotted as a function of 1/T in Fig. 5.2 From the slope and intercept of this plot, the standard enthalpy and entropy of solution were calculated to be - 236.4 ± 23.3 kJ/mol and 65.3 ± 8.3 J/K mol, respectively Using these quantities, the solubility of nitrogen in liquid Nb can be represented as a function of temperature and partial pressure of nitrogen as follows

$$\log C_N = \frac{12330}{T} - 3.41 + 1/2 \log P_{N_2} \quad (< \sim 2 \text{ wt.\%}) \tag{5.4}$$

where C_N is in wt.%, T is in K, and P_{N_2} is in atm. It must be emphasized that Equation (5.4) is valid only in the range where Sieverts law is applicable This is

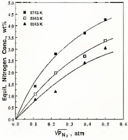

Fig. 5.1 Plot of equilibrium concentration as a function of $P_{N_2}^{1/2}$ at various temperatures

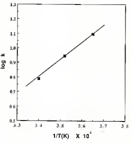

Fig. 5.2 Arrhenius type plot of log k, Sievert constant, versus 1/T

slightly different from the solubility data at 2800 K reported by Revyakin and al[76Rev]. For example, the solubility of N at 2800 K under 0.03 atm nitrogen partial pressure is calculated to be 10.3 at.% according to equation (5.4) while the calculated value at the same conditions according to their solubility equation was 7.9 at. %. The discrepancy may perhaps be due, at least in part, to the errors in the measurements of temperature, partial pressure, and compositions.

Reaction Sequence

Since nitrogen absorption in liquid Nb is a heterogenous process, it can be considered to occur in the following five distinct elementary steps, as shown schematically in Fig. 5.3. Each elementary step and its rate equation can be described as follows.

(1)gas phase transport

(i)transport of nitrogen molecules from the gas phase to the gas/metal interface.

$$N_2(b) \quad -> \quad N_2(i)$$

$$r = k_g\ (A/V)(P_{N_2(b)} - P_{N_2(i)}) \tag{5.5}$$

(2)chemical reactions

(ii)adsorption of nitrogen molecules on the metal surface

$$N_2(i) + v \quad <=> \quad N_2^*$$

$$r = (A/V)(k_2\ P_{N_2(i)}\ C_v - k_2'\ C_{N_2^*}) \tag{5.6}$$

(iii)dissociation of the adsorbed molecules into adsorbed atoms

$$N_2^* + v \quad <=> \quad 2\ N^*$$

$$r = (A/V)(\ k_3\ C_{N_2^*}\ C_v - k_3'\ C_{N^*}^2) \tag{5.7}$$

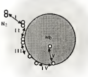

Fig. 5.3 Reaction mechanism of nitrogen absorption/desorption in liquid Nb

I Gas phase transport
II Adsorption of nitrogen molecule on the liquid surface
III Dissociation of adsorbed nitrogen molecules into atoms
IV Incorporation of the adsorbed atom to subsurface layer
V Liquid phase transport

(iv)incorporation of the adsorbed atoms to subsurface layers, and

$$N^* \Leftrightarrow N(i) + v$$

$$r = (A/V)(k_i C_{N^*} - k_i' C_{N(i)} C_v) \qquad (5.8)$$

(3)liquid phase transport

(v)transport of nitrogen atoms to bulk metal.

$$N(i) \rightarrow N(b)$$

$$r = k_l(A/V)(C_{N(i)} - C_{N(b)}) \qquad (5.9)$$

In the foregoing, the 'b' and 'i' denote the quantities in the bulk and at the surface, v and C_v stand for a vacant site available for reaction and the concentration of vacant site, respectively. The * indicates the entities adsorbed on the surface. k_g, k_l, k_i, and k_i' are the mass transfer coefficient in the gas phase, the mass transfer coefficient in the liquid phase, the rate constant for forward reaction, and the rate constant for backward reaction respectively, A is the specimen surface area, and V is the melt volume. It is to be noted that the rates of elementary steps (ii), (iii) and (iv) are expressed as the difference between a rate in the forward reaction and an opposing rate because each elementary reaction is reversible. In contrast, rate equations for steps (i) and (iv) are formulated as (rate constant) x (driving force) based on the fact that both processes are basically diffusion controlled in the boundary layer.

In the desorption reaction the same steps occur in the reverse sequence. Of the various elementary steps list above, the slowest one or a combination of steps will control the overall reaction rate. Thus, characteristics of each step will be discussed in some detail in the following section.

Characteristics of Each Elementary Step

Gas phase transport

If the rate of nitrogen absorption is controlled by the gas phase transport, the followings are anticipated based upon the discussion given in the previous chapter

1. The nitrogen absorption would be a second order with respect to nitrogen concentration or directly proportional to the nitrogen partial pressure
2. The rate of nitrogen absorption would be influenced by the flow rate of input gas stream because gas phase mass transfer coefficient is a function of Reynold number which includes the velocity term.
3. The apparent activation energy would be small, i.e., between 1 and 4 kcal/mol.[68Med]

Adsorption of nitrogen molecule

If the adsorption of nitrogen molecules on the surface, step(ii), is the rate controlling step, then the overall reaction rate will be dominated by the rate of nitrogen molecules adsorption. In other words, all other steps are virtually in equilibrium or very rapid. The rate equation in this case can be written as

$$r = (A/V)(k_2 P_{N_2(i)} C_v \quad k_2' C_{N_2}') \qquad (5.6)$$

By assumption, it implies that

(1) gas phase transport is very rapid.

$$P_{N_2(b)} = P_{N_2(i)} = P_{N_2} \qquad (5.10)$$

(2) dissociation step is at virtual equilibrium.

$$K_3 = k_3/k_3' = (C_{N^*}^2/C_{N_2^*} C_v) \qquad (5.11)$$

(3) dissolution step is also at virtual equilibrium.

$$K_4 = k_4/k_4' = (C_{N(i)}C_v/C_{N^*}) \qquad (5.12)$$

(4) liquid phase transport is very fast.

$$C_{N(i)} = C_{N(b)} = C_N \qquad (5.13)$$

where 'K$_i$'s are equilibrium constants for each substep. Substituting equations (5.10) – (5.13) into equation (5.6), it yields

$$r = (A/V)(k_2 P_{N_2} C_v - (k_2'/K_3 K_4)C_v C_N^2) \qquad (5.14)$$

If the equilibrium constant for overall nitrogen absorption is denoted by K, then

$$K = K_2 K_3 K_4^2 = C_{Ne}^2 / P_{N_2} \qquad (5.15)$$

Using equation (5.15), equation(5.14) can be further reduced.

$$r = (A/V)(k_2/K)C_v(C_{Ne}^2 - C_N^2) \qquad (5.16)$$

Equation(5.16) is the rate equation in case the adsorption of nitrogen molecule on the surface is the rate controlling step. It follows from the equation that the rate of nitrogen absorption must exhibit a second order dependence with respect to nitrogen concentration in the melt if the overall reaction rate is indeed controlled by step (ii).

Dissociation of adsorbed nitrogen molecules into atoms

When the dissociation of adsorbed nitrogen molecules into atoms is the rate controlling step, the rate of nitrogen absorption is given by

$$r = (A/V)(k_3 C_{N_2^*} C_v - k_3' C_{N^*}^2) \qquad (5\ 7)$$

In a similar way, the interfacial and adsorbed quantities may be eliminated from equation(5.7). The rate equation is then written as follows

$$r = (A/V)(k'_3 C_v^2/K_a)(C_{Ns}^2 - C_N^2) \qquad (5.17)$$

From the above equation, it is seen that the rate of nitrogen absorption is also second order with respect to nitrogen concentration if overall reaction is controlled by the dissociation of nitrogen molecules at the surface

Dissolution of nitrogen atoms into liquid phase

The adsorbed nitrogen atoms must dissolve in the liquid phase in order for the nitrogen absorption to proceed. If the dissolution of nitrogen atoms is the rate controlling step, then the rate equation is

$$r = (A/V)(k_4 C_{N*} - k_4' C_{N(l)} C_v) \qquad (5.8)$$

The elimination of the interfacial and adsorbed quantities from equation (5.8) by using the concept of virtual equilibrium results in the following equation.

$$r = (A/V)\, k_4' C_v\, (C_{Ns} - C_N) \qquad (5.18)$$

According to equation (5.18), the overall reaction is first order with respect to nitrogen concentration if dissolution of nitrogen atom in liquid is rate controlling step

Liquid phase transport

If the nitrogen absorption is controlled by the liquid phase transport, the rate of nitrogen absorption will then be given by

$$r = (A/V)\, k_l\, (C_{Ns} - C_N) \qquad (5.9)$$

This equation shows a first order dependence with respect to the nitrogen concentration. Also, liquid phase mass transfer coefficient, k_s, will be affected by the change of hydrodynamic condition in the liquid droplet.

So far, several rate equations have been developed for the elementary step which is assumed to be rate controlling. Each rate equation permits certain predictions which must be realized if the elementary step underlying the rate equation is indeed the rate controlling step. Those are summarized in Table 9.

The Order of Reaction and Rate Controlling Step

Based upon the characteristics of each elementary step as a rate controlling step, it is possible to determine the order of reaction and the rate controlling step in the nitrogen absorption reaction. As can be seen in Table 9, the reaction will have the first or the second order dependence with respect to nitrogen concentration depending on the elementary step. The two types of process can be represented as follows.

First-order reaction

$$\frac{dC_N}{dt} = k_1 \frac{A}{V} \left(C_{Ne} - C_N \right) \tag{5.19a}$$

or integrated form of equation(5.19a) is

$$- \ln \left(\frac{C_{Ne} - C_N}{C_{Ne} - C_{No}} \right) = k_1 \frac{A}{V} t \tag{5.19b}$$

Second-order reaction

$$\frac{dC_N}{dt} = k_2 \frac{A}{V} \left(C_{Ne}^2 - C_N^2 \right) \tag{5.20a}$$

or integration of equation(5.20a) gives

Table 9 Summary of the characteristics of each elementary step as a rate controlling step

Elementary step	Flow rate	nitrogen partial pres	nitrogen conc.	hydrodynamics in liquid
Gas phase transport	O	$\propto P_{N_2}$	$\propto C_N^2$	X
Adsorption of N_2 molecules	X	$\propto P_{N_2}$	$\propto C_N^2$	X
Dissociation	X	$\propto P_{N_2}$	$\propto C_N^2$	X
Dissolution	X	$\propto P_{N_2}^{1/2}$	$\propto C_N$	X
Liquid phase transport	X	$\propto P_{N_2}^{1/2}$	$\propto C_N$	O

O, some effect X no effect

$$\frac{1}{2C_{N_e}} [\ln (\frac{C_{N_e} + C_N}{C_{N_e} - C_N}) + \ln (\frac{C_{N_e} - C_{N_0}}{C_{N_e} + C_{N_0}})] = k_2 \frac{A}{V} t \qquad (5.20b)$$

where C_N, C_{N_0} and C_{N_e} are nitrogen concentration at time t, at t = 0, and at equilibrium, respectively. A is the specimen surface area, V is the melt volume, and k_1 and k_2 are the first and second-order rate constant, respectively. Now, if gas phase transport (step(i)) is rate controlling, the overall rate will be second order and be affected by the change of the gas flow rate because mass transfer coefficient, k_g, is influenced by the gas velocity. Accordingly, with the same data as shown in Fig. 4.1, the second-order rate constants for each flow rate were calculated and plotted as a function of Reynolds number in Fig. 5.4. It is seen that the rate constant increases with increasing gas flow rate up to approximately 200 in Reynolds number beyond which it becomes essentially independent of the gas flow rate. This indicates clearly that at lower flow rates, the reaction rate is influenced by the gas flow velocity, implying that the gas phase mass transport controls the overall reaction rate. Physically, in this regime, gas boundary layer is so wide that the concentration gradient in this layer is quite small, leading to the slower reaction rate. As the flow rate increases further, the mass transport rate of nitrogen molecules keeps increasing because the concentration gradient is increased further, finally reaching a point at ≈ 200 in Reynolds number where the mass transfer rate in the gas phase is comparable to that of the other elementary steps. Beyond that point, the gas phase transport takes place faster than the other elementary steps. Consequently, the reaction control is transferred from step (i) to one or more of the other elementary steps, resulting in the observed non-dependence of the rate constant on the total

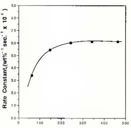

Fig 5.4 Effect of gas flow rate on the second order rate constant for nitrogen absorption in liquid Nb

flow rate. It may be mentioned that the absorption/desorption data described previously were obtained at total flow rate of 480 in Reynolds number. Consequently, step (i) is not expected to have any controlling effect on the overall reaction kinetics.

In case step (v) is a rate controlling step, any change in hydrodynamics of the liquid phase will have a considerable effect on the rate of nitrogen absorption and rate equation should be first order. It is likely that vigorous convective motion present in the levitated liquid Nb droplet under electromagnetic field will greatly increase the mass transfer rate. This is supported by Rao and Lee's experiment[82Lee] on the diffusivity of carbon in an iron-carbon droplet where the carbon mass transfer in the liquid phase was enhanced by about ten times under electromagnetic conditions compared to a stationary condition. Consequently, step (v) is not expected to be a rate controlling step in the experimental system used in this investigation. This is further supported by these experiments which show that nitrogen absorption is not a first order.

In determining the rate controlling step among other three elementary steps it is necessary to compare the data obtained experimentally with theoretical rate laws. As summarized in Table 9, if step (ii) or (iii) is the rate limiting step, then the reaction is a second order process with respect to nitrogen concentration, while if step (iv) controls the overall reaction rate, then the reaction is a first-order process. It should be noted that the rate constants k_1 and k_2 in the equations (5.19a) and (5.20a) are constant at a given temperature because three elementary steps of consideration are chemical processes. In order to determine if the overall reaction is first-order or not, the absorption data collected at 2743, 2843, and 2943 K under various partial pressures of nitrogen are plotted in Fig. 5.5 using Equation (5.19b). In this figure, the slopes indicate the rate constant, k_1. It can be seen that in each case, the data are split into three or four distinct lines, each representing a different partial pressure of N_2 in the gas mixture. If the overall reaction is first-order, the data obtained at a given temperature should fall on one line irrespective of the nitrogen partial pressure because the rate constant is determined by the reaction temperature only. Accordingly, this finding suggests that the rate controlling step for nitrogen absorption in liquid Nb is not first-order. This implies that the elementary step (iv) does not control the overall reaction.

In order to examine the possibility of a second-order reaction, the left hand side term in Equation (5.20b) was plotted as a function of (A/V)t for each reaction temperature. This is shown in Fig. 5.6 for temperatures of 2743, 2843, and 2943 K. It can be seen that within the limits of experimental error, the data in each case fall on a single straight line regardless of the N_2 partial pressure used. Thus, it is concluded that either elementary step (ii) or (iii), which are both second-order, must be controlling the overall reaction rate.

The data analysis for desorption experiments is exactly analogous because nitrogen desorption is expected to occur in reverse sequence. For the desorption data in Fig. 4.4, the first order and the second order plots were drawn in Fig. 5.7 and Fig. 5.8, respectively. In these figures, the initial concentration, C_{No}, and the equilibrium concentration, C_{Ne}, were taken from the absorption data obtained under the same processing conditions. The first order plot shows a splitting similar to that

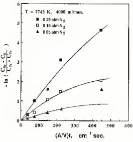

(a)

Fig. 5.5 Kinetics of nitrogen absorption into liquid Nb under various partial pressure of nitrogen correlated with first order rate equation

(a) 2743 K (b) 2843 K (c) 2943 K

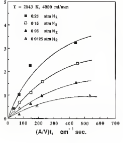
T = 2843 K, 4000 ml/min
■ 0.25 atm N_2
□ 0.15 atm N_2
▲ 0.05 atm N_2
△ 0.0125 atm N_2
$-\ln\left(\frac{C_{Ne} - C_{N}}{C_{Ne} - C_{No}}\right)$
0
1
2
3
4
5
0
100
200
300
400
500
600
700
(A/V)t_i cm^{-1} sec.

(b)

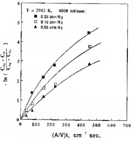
T = 2943 K, 4000 ml/min
■ 0.25 atm N2
□ 0.15 atm N2
▲ 0.05 atm N2
$-\ln\left(\frac{C_{Ne} - C_N}{C_{Ne} - C_{Ni}}\right)$
0
1
2
3
4
5
6
0
100
200
300
400
500
600
700
(A/V)t, cm⁻¹ sec.

(c)

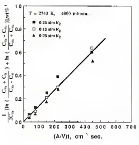

(a)

Fig. 5 6 Kinetics of nitrogen absorption into liquid Nb under various partial pressure of nitrogen correlated with second order rate equation

(a) 2743 K (b) 2843 K (c) 2943 K

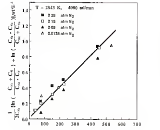
$T = 2843$ K, 4000 ml/min
■ 0.25 atm N_2
□ 0.15 atm N_2
▲ 0.05 atm N_2
△ 0.0125 atm N_2
$\frac{1}{2C_{Ne}}\{\ln(\frac{C_{Ne}+C_N}{C_{Ne}-C_N})+\ln(\frac{C_{Ne}-C_{No}}{C_{Ne}+C_{No}})\}$, wt%$^{-1}$
0.0
0.2
0.4
0.6
0.8
1.0
1.2
1.4
0
100
200
300
400
500
600
700
(A/V)t, cm^{-1} sec.

(b)

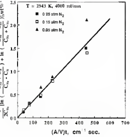
T = 2943 K, 4000 ml/min
■ 0 25 atm N_2
□ 0 15 atm N_2
▲ 0.05 atm N_2
$\frac{1}{2C_{Ns}}[\ln(\frac{C_{Ns}+C_N}{C_{Ns}-C_N})+\ln(\frac{C_{Ns}-C_{Ns}}{C_{Ns}+C_{Ns}})]$, wt%$^{-1}$
0 0
0.5
1 0
1.5
2 0
2.5
0
100
200
300
400
500
600
700
(A/V)t, cm^{-1} sec.

(c)

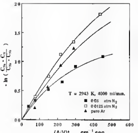

Fig. 5.7 Kinetics of nitrogen desorption from liquid Nb under various partial pressures of nitrogen correlated with first order rate equation

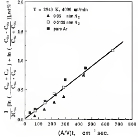

Fig. 5.8 Kinetics of nitrogen desorption from liquid Nb under various partial pressures of nitrogen correlated with second order rate equation

in absorption, while the data correlate well with the second-order plot. Based on this analysis, it can be concluded that the desorption reaction is again controlled by elementary steps (ii) or (iii).

Reaction Rates of Nitrogen Absorption and Desorption

Since the nitrogen absorption process was found to be second order, the apparent activation energy for nitrogen absorption can be deduced from the temperature dependence of the second order rate constant. The Arrhenius type plot for the second order rate constants are shown in Fig. 5.9. The apparent activation energy was calculated to be 327.2 ± 20.6 kJ/mole from the slope and preexponential constant, k_o, was $2.29 \cdot 10^6$ from the intercept. Therefore, the rate equation can be expressed as

$$\left(\frac{dC_N}{dt} \right)_{abs} = 2.290 \cdot 10^6 \exp\left(- \frac{39200}{T} \right) \frac{A}{V} \left(C_{Ne}^2 - C_N^2 \right) \qquad (5.21)$$

for 2700 K to 3000 K

where C_N and C_{Ne} are the nitrogen concentration and equilibrium nitrogen concentration, respectively, in wt %, A is the surface area in Cm^2, V is the volumn in Cm^3, T is the temperature in K.

Temperature dependance of the desorption rate can be derived by making use of the values of the solution enthalpy, - 236.4 kJ/mole, and the second order rate constant for the desorption process at 2943 K, a value of which was obtained to be $1.820 \cdot 10^3$ from the slope in Fig. 5.9. As mentioned earlier, the nitrogen solution reaction in liquid Nb is reversible and found to be exothermic. Thus the apparent activation energy for desorption should be larger than that for the

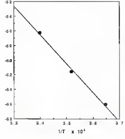

Fig 5.9 Effect of temperature on second order rate constant, k, of nitrogen absorption

absorption by the amount equal to solution enthalpy. Accordingly, the rate equation can be given by

$$\left(\frac{dC_H}{dt}\right)_{des} = 1.68 \cdot 10^{2} \exp\left(-\frac{67500}{T}\right) \frac{A}{V} (C_{He}^2 - C_H^2) \qquad (5.22)$$

for 2700 K to 3000 K

From the difference in activation energies for both processes, it can be predicted that desorption process takes place more slowly than absorption reaction under the same amount of concentration deviation from the equilibrium state. Such prediction is demonstrated well in that the calculated rate constant for absorption at 2943 K is $3.62 \cdot 10^{-3}$ which is larger than that for desorption process at the same temperature, $1.820 \cdot 10^{-3}$.

Carbon Monoxide

Solubilities of C and O under CO Atmosphere

In order to get the pressure-temperature-equilibrium concentrations relationship concerning CO- liquid Nb interaction, the values of $C_{Ce} \cdot C_{Oe}$, the multiplication of C and O equilibrium concentrations, obtained at 2813 K(from Fig. 4.6 and Fig. 4.7) were plotted as a function of P_{co} in Fig. 5.10. In view of the thermodynamics of dissolution of C and O, a linear relationship should arise when activities of C and O are used instead of the concentrations of each elements. A constant slope observed in this figure make it reasonable to assume that the activity coefficients of both elements are relatively constant in the range of temperature and partial pressures of CO used.

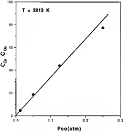

Fig 5 10 Relationship between equilibrium carbon and oxygen concentrations and partial pressure of CO

Temperature dependence of saturation concentrations are shown in Fig. 5.11 in which the value of Ln $C_{Cs} \cdot C_{Os}/P_{co}$ obtained at various temperature (from Fig. 4.8 and Fig. 4.9) were plotted versus 1/T. From the slope and the intercept in this graph, the P T C relationship in the saturated state was deduced to be

$$\ln C_{Cs} + \ln C_{Os} - \ln P_{co} = 2.32 \cdot 10^{4}/T - 2.35 \tag{5.23}$$

where P_{co} is in atm, and C_{Cs} and C_{Os} are in at %.

Reaction Sequence in CO - Liquid Nb Interaction

Some observations which might be useful in developing a kinetic model for C and O dissolutions in liquid Nb from CO gas are summarized as follows:

1. Both carbon and oxygen atoms from CO gas are dissolved into liquid Nb (Fig. 4.6 and Fig. 4.7)
2. The dissolution process proceeds with a relatively constant ratio of O to C of less than unity(= 0.76) over the entire run (Fig. 4.10)
3. There exists the saturated concentrations of C and O at a given partial pressure of CO and temperature.(Fig. 4.6 and Fig 4.7)
4. In desorption, the atomic O/C ratio of desorbed amounts is approximately unity (Fig. 4.18)

Based upon the above observations, it can be realized clearly that CO(gas) = C(in Nb) + O(in Nb) is the major reaction in the dissolution of C and O into liquid Nb from CO gas. However, the atomic O/C ratio less than the unity makes it necessary to determine how C surplus (or O deficiency) arises during the dissolution

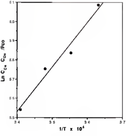

Fig. 5.11 Relationship between Ln($C_{Ce}C_{Oe}$/Pco) and 1/T

reaction. It can be speculated that there exists some side reaction(s) which causes the observed results. There are two possible reactions to explain such results.

i) $2\,CO \Leftrightarrow [C] + CO_2$ (5.24)

ii) $Nb + O \rightarrow NbO$

or $Nb + 2O \rightarrow NbO_2$ (5.25)

If reaction (i) is taken as a side reaction, it would provide another source for carbon dissolution which can cause carbon surplus. Thermodynamic equilibrium of reaction (i) indicates that reaction (i) at 2773 K can takes place in the forward direction only when P_{co}/P_{co_2} is greater than ≈ $2.5 \cdot 10^7$ under the present processing conditions. Since the CO gas used in this experiment(initially P_{co}/P_{co_2} is $6.7 \cdot 10^4$) is expected to have much low P_{co}/P_{co_2} ratio even after passage through an ascarite column, reaction(i) can be discarded among the possibilities to explain the observed behavior. In addition, this view is also supported by the observation that CO_2 pressure remains almost constant during the entire processing period as shown in Fig. 4.12. Next, suppose that reaction(ii) occurs as a side reaction. Then, oxygen loss will result from the evaporation of niobium oxide(s), leading to the oxygen deficiency even if the same amount of adsorbed oxygen and carbon are generated from the major reaction, $CO(g) \rightarrow [C] + [O]$. Since vapor pressure of niobium oxides is known to become significant for oxygen desorption through niobium oxides evaporation at temperature above approximately 1900 K and oxygen pressure greater than 10^{-5} atm [72Fro1, 80Fro, 81Sch1], reaction(ii) seems to be the most possible side reaction to explain the O/C ratio less than unity

For the desorption process, on the other hand, the atomic ratio of O/C of about unity in the desorbed amounts indicates that simultaneous escape of C and O occurs through CO evolution, excluding the possibility of the decrease of oxygen concentration through the path of oxide evaporation. The difference in mechanisms between absorption and desorption can be explained as follows during the absorption, CO molecules are adsorbed on the Nb surface and dissociated into C and O atoms The adsorbed carbon is dissolved into the liquid metal In contrast, for the adsorbed oxygen, there are two competing paths, say, dissolution into liquid Nb or desorption through niobium oxide evaporation Of both paths, it is surmised, based on the observed O/C ratio of 0.76 in the samples, that the dissolution path is dominant over the oxide evaporation by approximately 4 times. For desorption process, on the other hand, the oxide evaporation and the recombination of C and O may be competing after the C and O atoms are transferred to the surface from the interior of liquid Nb The atomic O/C ratio of about unity in desorbed amount suggests that recombination process is dominant over the oxide evaporation to a great extent especially when carbon exists in excess initially This behavior seems to be closely related to the equilibrium vapor pressures of niobium oxide and CO in Nb-C O solution as shown in Fig 2 6 in which the vapor pressure of CO is two to three orders higher than that of niobium oxides over the niobium containing the same amounts of C and O It is also to be pointed out that the observed desorption mechanism is consistent with Ono and et al's works[80Ono] on the degassing of niobium containing carbon and oxygen in which only CO recombination occurs when carbon exists in excess whereas both CO recombination and niobium oxide evaporation take place together when oxygen exists in excess. Thus, it can be said that in absorption, CO dissolution is responsible for C and O absorption together with niobium oxide evaporation whereas in desorption only CO recombination path is taken for C and O desorption. Taking the discussion done so far into consideration the absorption and desorption paths can be visualized as shown in Fig. 5.12.

In the followings, a kinetic model on the interaction of liquid Nb with CO is made based upon the reaction CO(g) <=> [C] + [O] together with a side reaction of niobium oxide evaporation as shown schematically in Fig. 5.13. Each elementary step involved in this scheme can be described in the following way.

I. Gas phase transport

$$CO^b(g) \overset{r_1}{>} CO^i(g) \qquad (5.26)$$

II. Dissociative adsorption

$$CO^i(g) + 2v \underset{r_2'}{\overset{r_2}{<=>}} C^* + O^* \qquad (5.27)$$

III. Dissolution

a) Carbon dissolution

$$C^* \underset{r_{c1}'}{\overset{r_{c1}}{<=>}} C(i) + v \qquad (5.28)$$

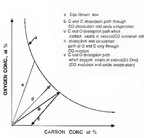
a Equilibrium line
b C and O absorption path through CO dissolution and oxide evaporation
c C and O desorption path when carbon exists in excess(CO evolution only)
d absorption and desorption path of O and C only through CO reaction
e C and O desorption path when oxygen exists in excess[82 Ono] (CO evolution and oxide evaporation)
a
e
d
b
c
OXYGEN CONC., at %
CARBON CONC at %

Fig. 5.12 Reaction paths during CO absorption and desorption

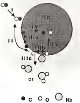

Fig. 5 13 Mechanism of carbon and oxygen dissolution in liquid Nb from CO gas
I. gas phase transport
II dissociative adsorption of CO
III a. carbon dissolution
b oxygen dissolution
c. niobium oxide evaporation
IV liquid phase transport

b) Oxygen dissolution

$$O^{*} \overset{r_{sd}}{\underset{r_{sd}'}{<=>}} O(i) + v \qquad (5.29)$$

c) Suboxides evaporation

$$O^{*} + Nb \xrightarrow{r_{NbO}} NbO + v \qquad (5.30)$$

$$2O^{*} + Nb \xrightarrow{r_{NbO_2}} NbO_2 + 2v \qquad (5.31)$$

IV Liquid phase transport

$$C(i) \xrightarrow{r_{lt}} [C] \qquad (5.32)$$

$$O(i) \xrightarrow{r_{lt}} [O] \qquad (5.33)$$

Hence, C^{*} and O^{*} denote chemisorbed C and O, respectively, C(i) and O(i) are dissolved species near subsurface of liquid Nb, v is a vacant surface site, and r_i is the reaction rate for an elementary step i. i, b, and [ ] indicate the near interface, the bulk, and the dissolved. It should be noted that step III-(c) is not included in reaction sequence of desorption because C and O desorption proceeds only through CO gas evolution as discussed previously. In this model, bound oxygen and carbon are assumed to be chemically adsorbed in an energetically common state. In some cases, physisorption of gas molecules as a precursor to atomic chemisorption is taken into consideration but the current scheme combines both steps into one. This is because the molecularly adsorbed gas intermediates are generally expected to have very short life time at high temperatures providing no real physical meaning as an independent substep[71Win1, 80Fro]. Another thing to be noted is that only two oxide forms via NbO(g) and $NbO_2(g)$ are taken into account and metal oxide evaporation is assumed to be an irreversible process. This assumption can be justified by the fact that the evaporating oxides are condensed on the glass wall continuously, making the backward reaction virtually negligible. Then the elementary reaction rate can be expressed in terms of elementary rate constants and relevant concentrations according to the mass action law as follows [74Ros, 76Ros]

$$r_1 = k_g(A/V)(P_m^b - P_m^s) \qquad (5.34)$$

$$r_2 = k_2(A/V)P_m^s(1 - \theta c - \theta o)^2 \qquad (5.35a)$$

$$r_2' = k_2'(A/V)\theta c\ \theta o \qquad (5.35b)$$

$$r_{a1} = k_{a1}(A/V)\theta c \qquad (5.36a)$$

$$r_{a1}' = k_{a1}'(A/V)(1 - \theta c - \theta o)\ C_{c(i)} \qquad (5.36b)$$

$$r_{a2} = k_{a2}(A/V)\theta o \qquad (5.37a)$$

$$r_{a2}' = k_{a2}'(A/V)(1 - \theta c - \theta o)\ C_{o(i)} \qquad (5.37b)$$

$$r_{3NbO} = k_{3NbO}(A/V)\theta o \qquad (5.38)$$

$$r_{3NbO_2} = k_{3NbO_2}(A/V)\theta o^2 \qquad (5.39)$$

$$r_{4c} = k_c(A/V)(C_{c(i)} - C_c) \qquad (5.40a)$$

$$r_{4o} = k_o(A/V)(C_{o(i)} - C_o) \qquad (5.40b)$$

where θc and θo are the fractional surface coverage of adsorbed C and O. A and V are surface area and volume of the sample, respectively, k_i is the rate constant for the step i, and C_c and C_o are concentrations of C and O species in the sample. Using the above equations, mass balance equations for the adsorbed species can be derived as

$$d\theta c/dt = r_2 - r_2' - r_{c3} + r_{c3}'$$

$$= (A/V)[\, k_2 P_{co}^{s}(1 - \theta c - \theta o)^2 - k_2'\theta c\, \theta o - k_{c3}\, \theta c + k_{c3}'(1 - \theta c - \theta o)\, C_{C(I)}] \qquad (5.41)$$

$$d\theta o/dt = r_2 - r_2' - r_{o3} + r_{o3}' - r_{NbO} - r_{NbO_2}$$

$$= (A/V)[\, k_2 P_{co}^{s}(1 - \theta c - \theta o)^2 - k_2'\theta c\, \theta o - k_{o3}\, \theta o + k_{o3}'(1 - \theta c - \theta o)\, C_{O(I)} - k_{NbO}\, \theta o - k_{NbO_2}\, \theta o^2\,] \qquad (5.42)$$

Steady state assumption of intermediates species gives $d\theta o/dt = 0$ and $d\theta c/dt = 0$.

The Order of Reaction and Rate Controlling Step in CO Absorption

As mentioned earlier, the gas flow rate does not affect the C and O absorption rates under the present experimental condition. Based upon the same explanation applied to Nb- N kinetics, it can be said that the transport in gas phase(step I) is not the rate controlling step, implying that $P_{co}^{b} = P_{co}^{i} = P_{co}$. This is because the rate of mass transfer in the gas phase is rapid enough compared with the rates of other steps, resulting in no concentration gradient in the boundary layer. The possibility of liquid phase transport as a rate controlling step may also be excluded using the same reasoning as in liquid Nb-N interaction. Thus, mathematically, it can be assumed reasonably that $C_{C(I)} = C_C$, and $C_{O(I)} = C_O$.

Suppose that dissolution step for carbon (III-a) and for oxygen (III-b) are the rate controlling step. The rate equations for C and O absorption can be then represented as

$$dC_C/dt = r_{c3} - r_{c3}'$$

$$= (A/V)[\, k_{c3}\, \theta c - k_{c3}'(1 - \theta c - \theta o)\, C_C] \qquad (5.43)$$

and

$$dC_O/dt = r_{o3} - r_{o3}'$$
$$= (A/V)[\, k_{o3}\, \theta o - k_{o3}'(1 - \theta c - \theta o)\, C_O] \qquad (5.44)$$

The above assumption implies that dissociative adsorption rate(step II) is so fast, compared with the net incorporation rate of C(step III-a) or O(step III-b), that step(II) is in virtual equilibrium state. So, the corresponding adatom coverage, θc and θo, are virtually constant at the coverage of quasi-equilibrium, θc* and θo*, throughout most of the absorption period. Therefore, carbon and oxygen dissolution rates in this case can be expressed as

$$dC_C/dt = (A/V)[\, k_{c3}\, \theta c^* - k_{c3}'(1 - \theta c^* - \theta o^*)\, C_C] \qquad (5.45)$$

and

$$dC_O/dt = (A/V)[\, k_{o3}\, \theta o^* - k_{o3}'(1 - \theta c^* - \theta o^*)\, C_O] \qquad (5.46)$$

On the other hand the net dissolution rates of C and O are zero in the quasi-equilibrium state, so that

$$dC_C/dt = (A/V)[k_{c3}\, \theta c^* - k_{c3}'(1 - \theta c^* - \theta o^*)\, C_{Ce}] = 0 \qquad (5.47)$$

and

$$dC_O/dt = (A/V)[k_{o3}\, \theta o^* - k_{o3}'(1 - \theta c^* - \theta o^*)\, C_{Oe}] = 0 \qquad (5.48)$$

where C_{Ce} and C_{Oe} are the concentrations of carbon and oxygen in equilibrium state, respectively. From equations (5.47) and (5.48), it can be derived that

$$(1 - \theta c^* - \theta o^*) = \frac{k_{c3}\, \theta c^*}{k_{c3}' C_{Ce}}$$
$$= \frac{k_{o3}\, \theta o^*}{k_{o3}' C_{Oe}} \qquad (5.49)$$

Inserting equation (5.49) into equations (5.45) and (5.46) gives

$$dC_C/dt = (A/V)[k_{c3}\,\theta c^* - k_{c3}'\,C_C\,(k_{c3}\,\theta c^* / k_{c3}' C_{Cs})]$$

$$= (A/V)[\frac{k_{c3}\,\theta c^*}{C_{Cs}}\,(C_{Cs} - C_C)]$$

$$= Kc(A/V)(C_{Cs} - C_C) \qquad (5.50a)$$

or in integrated form,

$$\ln\left(\frac{C_{Cs} - C_C}{C_{Cs} - C_{Co}}\right) = Kc\,\frac{A}{V}\,t \qquad (5.50b)$$

and

$$dC_O/dt = (A/V)[k_{o3}\,\theta o^* - k_{o3}'\,C_O\,(k_{o3}\,\theta o^* / k_{o3}' C_{Os})]$$

$$= (A/V)[\frac{k_{o3}\,\theta o^*}{C_{Os}}\,(C_{Os} - C_O)]$$

$$= Ko(A/V)(C_{Os} - C_O) \qquad (5.51a)$$

or in integrated form,

$$\ln\left(\frac{C_{Os} - C_O}{C_{Os} - C_{Oo}}\right) = Ko\,\frac{A}{V}\,t \qquad (5.51b)$$

where $Kc = k_{c3}\,\theta c^*/C_{Cs}$ and $Ko = k_{o3}\,\theta o^*/C_{Os}$.

These equations (5.50a) and (5.51a) indicate that if step III is the rate controlling step, the overall reaction either for carbon dissolution or for oxygen dissolution will be first order with respect to C or O concentration, respectively

On the other hand, let's assume that dissociative adsorption(step II) controls the overall reaction Then rate equation is written as

$$dC_{C^*}/dt = dC_{O^*}/dt = r_2 - r_2' \qquad (5.52)$$

Hence, since $dC_C/dt = dC_{C^*}/dt$ and $dC_O/dt + dC_{NiO}/dt + dC_{NiO_2}/dt = dC_{O^*}/dt$, the rate equations for carbon and oxygen dissolution in this case are represented as

$$dC_O/dt = (A/V)[\ k_2\ P_{co}'(1 - \theta c - \theta o)^2 - k_2'\ \theta c\ \theta o] \quad (5.53)$$

and

$$dC_O/dt = (A/V)[\ k_2 P_{co}'(1 - \theta c - \theta o)^2 - k_2' \theta c \theta o - (k_{bao}\ \theta o + k_{baoa} \theta o^2)] \quad (5.54)$$

The assumption of step II being the rate controlling step implies that dissolution reactions(step III-a and III-b) are so fast that the virtual equilibrium between the adsorbed and the dissolved species are maintained. Thus, the following relationships should be satisfied.

$$K_{c1} = k_{c}/k_{c1}' = C_C(1 - \theta c - \theta o)/\theta c \quad (5.55)$$

and

$$K_{o1} = k_{o}/k_{o1}' = C_O(1 - \theta c - \theta o)/\theta o \quad (5.56)$$

Substitution of the equations (5.55) and (5.56) into the rate equation (5.53) yields

$$dC_O/dt = (A/V)[k_2\ P_{co}(1-\theta c-\theta o)^2 - k_2'\ C_C\ C_O(1-\theta c-\theta o)^2/K_{c1}\ K_{o1}] \quad (5.57)$$

Since the equilibrium constant for the overall reaction is related to equilibrium constants for each elementary step equilibrium concentrations of C and O and partial pressure of CO gas, we have

$$K = K_2\ K_{c1}\ K_{o1} = (k_2/k_2')(k_c/kc_1')(k_o/k_{o1}') = C_{Ce}\ C_{Oe}/\ P_{co} \quad (5.58)$$

Substituting the relationship (5.58) in equation (5.57) gives

$$\begin{aligned} dC/dt &= (A/V)[k_2\ (1-\theta c-\theta o)^2(C_{Ce}\ C_{Oe})/K - k_2'K_2(C_C\ C_O)(1-\theta c-\theta o)^2/K] \\ &= (k_2/K)(A/V)(1-\theta c-\theta o)^2(C_{Ce}\ C_{Oe} - C_C\ C_O) \\ &= k_a'(A/V)(C_{Ce}\ C_{Oe} - C_C\ C_O) \end{aligned} \quad (5.59)$$

where k_a' is $(k_2/K)(1-\theta c-\theta o)^2$

The constancy of O/C atomic ratio as observed in the experimental results indicates

$$dC_o/dC_c = \frac{dC_o/dt}{dC_c/dt}$$

$$= \frac{[k_2P_m^{\ 1}(1 - \theta c - \theta o)^2 - k_2'\theta c\theta o] - (k_{MnO}\ \theta o + k_{MnO_2}\theta o^2)}{k_2\ P_m^{\ 1}(1 - \theta c - \theta o)^2 - k_2'\theta c\ \theta o}$$

$$= 1 - \frac{(k_{MnO}\ \theta o + k_{MnO_2}\theta o^2)}{k_2\ P_m^{\ 1}(1 - \theta c - \theta o)^2 - k_2'\theta c\ \theta o}$$

$$= \text{constant} \tag{5 60}$$

From the equation(5 60), it can be realized that ($k_{MnO}\ \theta o + k_{MnO_2}\ \theta o^2$) should be always a constant fraction of [$k_2\ P_m^{\ 1}(1 - \theta c - \theta o)^2 - k_2'\theta c\ \theta o$]. Thus, equation (5.54) can be written as

$$dC_o/dt = K'(A/V)(k_2\ P_m^{\ 1}(1 - \theta c - \theta o)^2 - k_2'\theta c\ \theta o) \tag{5 61}$$

where K' is the unity less the value of the ratio ($k_{MnO}\ \theta o + k_{MnO_2}\theta o^2$)/[$k_2P_m^{\ 1}(1 - \theta c - \theta o)^2 - k_2'\theta c\theta o$]

Thus, it is seen that the rate equation for oxygen dissolution is exactly the same form as that for carbon dissolution Using the same procedure for dC_c/dt, equation (5 61) yields

$$dC_o/dt = k_o'(A/V)\ (\ C_{C_e}\ C_{O_e} - C_C\ C_O\ ) \tag{5 62}$$

where $k_o' = K'k_c'$ Based upon the equations (5 59) and (5 62), it can be said that if the dissociative adsorption (step II) is controlling the overall reaction, both carbon and oxygen dissolution rate should be second order with first order dependence on C_c and C_o, respectively

In order to determine the order of reaction and thereby the rate controlling step, the absorption data collected at 2813 K under various partial pressures of CO are plotted in Fig 5 14 for carbon and Fig 5 15 for oxygen using the integrated form of the first order rate equations (5.50b) and (5 51b) It can be seen that in

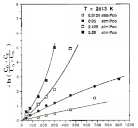

Fig. 5.14 Carbon absorption kinetics correlated with first order rate equation

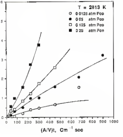

Fig. 5.15 Oxygen absorption kinetics correlated with first order rate equation

each case, the data are split into four distinct lines, each representing a different partial pressure of CO. Based upon the same reasoning as in nitrogen, this behavior suggests that the rate controlling step in C and O absorption in liquid Nb is not first-order, implying that the elementary step III does not control the overall reaction.

For the possibility of a second-order reaction, the equation (5.59) and (5.62) should be integrated to plug the data into it directly. Taking into consideration that the ratio of O to C is constant during the absorption period, both equations can be transformed into the equations (5.63a) and (5.64a) which are just common form of second order rate equations

$$dC_C/dt = k_c'(A/V)(C_{Co}\,C_{Oo} - C_C\,C_O)$$

$$= k_c\,(A/V)(\,C_{Co}^2 - C_C^2\,) \qquad (5.63a)$$

or in integrated form,

$$\frac{1}{2C_{Co}}\,[\ln\,(\,\frac{C_{Co} + C_C}{C_{Co} - C_C}) + \ln\,(\,\frac{C_{Co} - C_{Ci}}{C_{Co} + C_{Ci}})] = k_c\,\frac{A}{V}\,t \qquad (5.63b)$$

and

$$dC_O/dt = k_o'(A/V)\,(\,C_{Co}\,C_{Oo} - C_C\,C_O\,)$$

$$= k_o\,(A/V)\,(\,C_{Oo}^2 - C_O^2\,) \qquad (5.64a)$$

or in integrated form,

$$\frac{1}{2C_{Oo}}\,[\ln\,(\,\frac{C_{Oo} + C_O}{C_{Oo} - C_O}) + \ln\,(\,\frac{C_{Oo} - C_{Oi}}{C_{Oo} + C_{Oi}})] = k_o\,\frac{A}{V}\,t \qquad (5.64b)$$

where $k_c = 0.76\,k_c'$ and $k_o = k_o'/0.76$

Thus, the integrated forms of second order rate equations, (5.63b) for carbon and (5.64b) for oxygen were used in dealing with the absorption data. Fig. 5.16 and

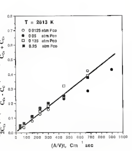

Fig. 5.16 Carbon absorption kinetics correlated with second order rate equation

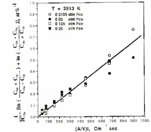

Fig 5 17 Oxygen absorption kinetics correlated with second order rate equation

Fig. 5.17 show the second order plot for C and O data at 2813 K in which it can be seen that the data representing the different partial pressure of CO fall on a single straight line within the limits of experimental error. Thus, it can be said that elementary step II is the rate controlling step for C and O dissolution into liquid Nb from CO gas.

Temperature Dependence of Absorption Rate Equation

Since the overall reaction is controlled by dissociative adsorption, which is second order, temperature dependence of the reaction rate can be derived by examining the temperature dependence of the second order rate constant k_c in equation(5.63b). Fig. 5.18 shows the second order plot for the data obtained at different temperatures. It is seen that the data collected at a given temperature falls on a single line without significant deviation. Taking the second order rate constant at each temperature(from the slopes in Fig. 5.18), an Arrhenius type plot of those values were made in Fig. 5.19. Based on the values of the slope and the intercept(Table 10), the rate equation for the absorption in liquid Nb is obtained as

$$(dC_C/dt)_{ads} = 12.1(A/V)\exp(-26700/T)(C_{Ce}C_{Oe} - C_C C_O) \qquad (5.65)$$

where C_C and C_O are in at %, A is in Cm², V is in Cm³, and T is in K.

It is to be noted that the k_c value obtained in this plot is 0.76 k_c' because the value of O concentration is replaced with the value of C concentration in calculation for the second order plot. Since O/C ratio remains constant at 0.76 during the entire dissolution process, the oxygen absorption rate can be represented as

$$(dC_O/dt)_{ads} = 9.20(A/V)\exp(-26700/T)(C_{Ce}C_{Oe} - C_C C_O) \qquad (5.66)$$

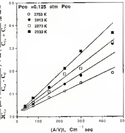

Fig. 5.18 Second order plot of carbon absorption data at various temperatures

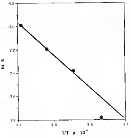

Fig 5 19 Arrhenius type plot of second order rate constants on carbon absorption in CO atmosphere

Table 10 Apparent activation energies on CO–liquid niobium reaction

	slope (Q/R)	intercept(ln k_o)
Absorption	26700	2.23
Desorption	47500	10.55

* The values are taken from Fig. 5.19 and Fig. 5.23

The Order of Reaction and Rate Equation for CO Desorption

In the analysis of desorption data, the strategy is basically analogous to absorption data analysis although oxygen desorption does not occur through oxide evaporation It is expected that desorption rates of both elements are the same. However, it is more convenient to take the oxygen data instead of carbon because desorption process through CO evolution lead to carbon residue when carbon exists in excess at the beginning of desorption The oxygen desorption data in Fig 4 14 is plotted in Fig 5 20 and Fig. 5 21, respectively, in accordance with the integrated form of equations (5 51b) and (5 64b). The first-order plot shows a splitting similar to that in absorption, while the data are correlated well with the second-order plot. This behavior implies that the desorption reaction is again controlled by elementary step II

To investigate how desorption rate is varied with temperature, the second order plot is drawn in Fig 5.22 for the desorption data of oxygen obtained at various temperatures In this plot, the modified integrated form of second order rate equation, equation (5 67), is utilized assuming that partial pressure of oxygen in pure Ar is zero.

$$1/C_O - 1/C_{Oo} = k(A/V)t \qquad (5\ 67)$$

Taking the rate constants, k, at each temperature from Fig 5 22 (slopes), the value of ln k is plotted against 1/T in Fig 5 23 Based upon the values of slope and intercept(Table 10), the rate equation for the desorption process can be expressed as follows

$$(dC_O/dt)_{de} = (dC_C/dt)_{de} = 3\ 80{\cdot}10^4(A/V)\ \exp(-47500/T)(\ C_{Ce}\ C_{Oe} - C_C\ C_O\ ) \qquad (5\ 68)$$

where C_C and C_O are in at %, A is in Cm^2, V is in Cm^3, and T is in K

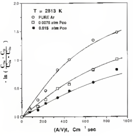

Fig 5 20 First order plot of oxygen desorption kinetics in atmospheres with various partial pressures of CO

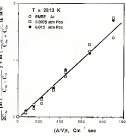

Fig. 5.21 Second order plot of oxygen desorption kinetics in atmospheres with various partial pressures of CO

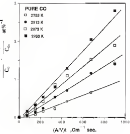

Fig. 5.22 Second order plot of oxygen desorption data in pure Ar atmosphere obtained at various temperatures

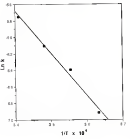

Fig 5 23 Plot of Ln k, second order rate constant of oxygen desorption in pure Ar, versus 1/T

CHAPTER 6
CONCLUSION

Using an electromagnetic levitation technique, absorption and desorption behaviors of nitrogen and carbon monoxide in liquid niobium were investigated under various experimental conditions of temperature, partial pressure, gas flow rate, and the processing time. Some important results are as follows.

Interaction of nitrogen with liquid Nb

1. Nitrogen solution reaction in molten niobium is exothermic with standard solution enthalpy and entropy of -236.4 kJ/mol and - 65.3 J/K mol, respectively. The solubility of nitrogen can be represented as a function of the nitrogen partial pressure and temperature as follows:

   $$\log C_N = \frac{12330}{T} - 3.41 + 1/2 \log P_{N_2} \qquad (<= 2 \text{ wt.\%})$$

   where C_N is in wt.%, T is in K, and P_{N_2} is in atm.

2. In the present experimental set-up the gas flow rate can affect the nitrogen absorption kinetics up to approximately 200 in Reynolds number, while beyond that value, absorption rate was independent of the gas flow rate.

3. Both absorption and desorption of nitrogen in molten niobium are second-order processes with respect to the nitrogen concentration. The rate controlling step in the absorption process is expected to be either the

adsorption of nitrogen molecules on the liquid surface or the dissociation of nitrogen molecules into nitrogen atoms

4 The rate equations for absorption and desorption are expressed as

$$\left(\frac{dC_N}{dt}\right)_{abs} = 2.290 \cdot 10^5 \exp\left(-\frac{39200}{T}\right)\frac{A}{V}(C_{Ne}^2 - C_N^2)$$

for 2700 K to 3000 K.

and

$$\left(\frac{dC_N}{dt}\right)_{des} = 1.680 \cdot 10^7 \exp\left(-\frac{67500}{T}\right)\frac{A}{V}(C_{Ne}^2 - C_N^2)$$

for 2700 K to 3000 K

where C_N is in wt.%, A is in Cm², V is in Cm³, T is in K.

Interaction of carbon monoxide with liquid Nb

5 C and O solution reaction in liquid Nb is also exothermic The relationship of P-T-C_{Ca}·C_{Oa} is given by

$$\ln C_{Ca} + \ln C_{Oa} - \ln P_{co} = 2.32 \cdot 10^4/T - 2.35$$

where P_{co} is in atm , C_{Ca} and C_{Oa} are in at %

6 During absorption of CO, C and O dissolution reaction is working together with the evaporation of niobium oxide, maintaining the constant C_O/C_C ratio less than unity over the entire absorption period. In contrast, in desorption process, only CO evolution reaction is responsible for the decrease of C and O concentrations, leading to C_O/C_C ratio of about unity especially when excess carbon exists at the initial sample

7 Based upon a proposed kinetic model both absorption and desorption processes are second order with the first order dependence on C_C and C_O.

respectively, implying that the overall reaction rate is controlled by the substep of dissociative adsorption (or recombination of C and O in the case of desorption)

8. The rate equations for C/O absorption and desorption are found to be

$$(dC_C/dt)_{ads} = (1/0.76)(dC_O/dt)_{ads} = 12.1(A/V)\exp(-26700/T)(C_{Co}\,C_{Oo} - C_C\,C_O)$$

and

$$(dC_C/dt)_{des} = (dC_O/dt)_{des} = 3.80 \cdot 10^4(A/V)\exp(-47500/T)(\,C_{Co}\,C_{Oo} - C_C\,C_O\,)$$

where C_C and C_O are in at %, A is in Cm^2, V is in Cm^3, and T is in K

REFERENCES

[36Rei] A. Reimann and C. K. Grant, Phil. Mag., 1936, 22, p.34

[53Ang] Choh-Yi Ang and C. Wert, J. Met., 1953, 5, p.1032.

[59Spe] R. Speiser, P. Blackburn and H. L. Johnston, J. Electrochem. Soc., 1959, 106, p.52

[60Beg] R. T. Begley and W. N. Platte, WADC Tech. Rep., Part 4, 1960

[60Ell] R. P. Elliott, Trans. ASM, 1960, 52, p.990.

[60Ste] R. L. Steinberger and R. E. Treybal, AIChE Journal, 1960, 6, no.2, p.227

[60Win] O. Winkler, Metall. Rev., 1960, 5, p.1

[62Bre] L. Brewer and G. Rosenblatt, Trans. Met. Soc. AIME, 1962, 224, p.1268

[63Des] W. DeSorbo, Phys. Rev., 1963, 132, p.107

[63Geb] E. Gebhardt, and R. Rothenbacher, Z. Metallkd., 1963, 54, p.443

[63Peh] R. D. Pehlke and J. F. Elliott, Trans. Met. Soc. AIME, 1963, 218, p.1088

[64Geb] E. Gebhardt, E. Fromm and D. Jakob, Z. Metallkd., 1964, 55, p.432.

[65Fro1] E. Fromm and H. Jehn, Z. Metallkd., 1965, 56, p.599

[65Fro2] E. Fromm and H. Jehn, Brit. J. Appl. Phys., 1965, 16, p.653

[65Kof] P. Kofstad and S. Espevik, J. Electrochem. Soc., 1965, 112, p.153

[65Pas] R. A. Pasternak and B. Evans, J. Electrochem. Soc., 1965, 112, p.153

[65Pei] W. A. Peifer, J. Met., 1965, 17, p.487

[66Geb] E. Gebhardt, W. Durrschnabel and G. Horz, J. Nucl. Mater., 1966, 18, p.149

[66Hor1] G Horz, Z. Metallkd., 1966, 57, p 703

[66Hor2] G Horz and E Gebhardt, Z. Metallkd., 1966, 57, p.737

[66Wis] C D Wiseman, J. Appl. Phys., 1966 37, p 3599

[67Bak[L. A Baker, N A Warner and A. E. Jenkins, Trans. Met. Soc. AIME, 1967, 239, p 857

[67Pas] R A Pasternak, and B Evans, J. Electrochem. Soc., 1967, 14, p.452

[67Swi] J H Swisher and E. T Turkdogan, Trans. Met. Soc. AIME, 1967, 239, p.602.

[68Dis] P A Distin, G D Hallett and F D Richardson, J. Iron Steel Inst, 1968, p 821

[68Fro1] E Fromm, J. Less-Common Met, 1968 14, p 113

[68Fro2] E. Fromm and G Spaeth, Z. Metallkd, 1968, 59, p.65

[68Hor1] G Horz, Z. Metallkd., 1968, 59, p 180.

[68Hor2] G Horz, Z. Metallkd., 1968, 59, p 283

[69Eva] J H. Evans and B H. Eyre, Acta Metall., 1969, 17, p.1109

[69Fro] E Fromm and H Jehn Vacuum, 1969, 19, p 191

[70Els] G Elssner and G Horz, J. Less-Common Met., 1970, 21, p 451

[70Fen] H. H Feng, 1975, Ph D dissertation, Yale University

[70Fro1] E. Fromm, J. Vac. Sci. and Tech., 1970, 7, p s100

[70Fro2] E. Fromm, J. Less-Common Met. 1970, 22, p 139

[70Gle] C. G Glen and F D Richardson,"Heterogeneous Kinetics at Elevated Temperatures," eds G R Belton and W L. Worrell, 1970 Plenum Press New york, London, p 369

[70Hor] G Horz and E Gebhardt, Werkst. Korros., 1970, 21, p. 995

[70Jeh] H. Jehn and E. Fromm, J. Less-Common Met., 1970, 21, p 333

[70Wag] C Wagner, 'Advances in Catalysis," 1970, vol 21, Academic Presss, New York and London, p.321

[70Win] O Winkler, J. Vac. Sci. and Tech., 1970, 7, p.514

[71Boc] E S Bocian Jr., and F Y Young, J. Electrochem. Soc., 1971, 118, p 2021

[71Fro1] E Fromm, Vacuum, 1971, 21, no.12 p 585

[71Fro2] E Fromm and H Jehn, High. Temp. High Press., 1971, 3 p.553

[71Fru] R. J Fruehan and L. J Martonik, High Temp. Sci., 1971, 3, p.244

[71Hor1] G Horz and E Steinheil, Z. Metallkd., 1971, 62, p 849

[71Hor2] G Horz and R Ziegeldorf, Z. Metallkd., 1971, 62, p 16

[71Mey] R W Meyerhoff, J. Electrochem. Soc., 1971, 118, no 6, p 997

[71Ric] F D Richardson Chem. Metall. of Iron and Steel, 1971, p 82

[71Win1] O Winkler, and R Bakish, 'Vacuum Metallurgy', 1971, Elservior, Amsterdam-London-New York, p 483

[71Win2] O Winkler, and R Bakish, 'Vacuum Metallurgy', 1971, Elsevior, Amsterdam-London-New York, p 7

[72Fro1] E. Fromm and H. Jehn, Metall. Trans.B 1972, 3, p 1685

[72Fro2] E Fromm and R Kirchheim, J. Less-Common Met., 1972, 26, p 403

[72Hor1] G Horz, Metall. Trans.B, 1972, 3, p 3069

[72Hor2] G Horz and K Lindenmaier Z. Metallkd., 1972, 63, p 97

[72Hor3] G. Horz and K. Lindenmaier, Z. Metallkd., 1972, 63, p 103

[72Hor4] G Horz and K. Lindenmaier, Z. Metallkd., 1972, 63 p.240

[72Ros] E Rosner, Annu. Rev. Mater. Sci., 1972, 2, p 573

[72Sol] M Y Solar and R. I L. Guthrie Metall. Trans.B 1972, 3, p 713

[72Szk] Z. C. Szkopiak, J. Less-Common Met., 1972, 26, p 9

[73Gio] S Giodano, H Hahn H. J Halama, C. Varmazis, and L. Rinderer, J. Appl. Phys., 1973, 44, p 4185

[73Hor1] G Horz and K Landenmaier, Z. Metallkd., 1973, 64, p 348

[73Hor2] G Horz, Metall., 1973, 27, p 680

[73Kle] M J Klein and A G Metcalfe, Metall. Trans. B, 1973, 4, p.2441

[73Rev] A. V Revyakin and L N Kozina. Russ. Metall., 1973, 5, p.251

[73Ros] D E. Rosner, E Steinheil, D P McArther, Metall. Trans., 1973, 4, p.2221

[74Ros] D E. Rosner, H. M Chung and H. H Feng, J. Chem. Soc. Faraday Trans. I, 1974, 72, p 842

[75Ros] D E Rosner, H H Feng and E Steinsheil,'Metal-Slag- Gas- Reaction and Processes," eds Z. A. Foroulis and W W Smeltzer, 1975, New Jersey, Electrochem. Soc p 548

[76Fro] E Fromm and E Gebhardt(ed)," Gase und Kohlenstoff in Metallen", Springer Verlag, Berlin, Heidelberg, New york, 1976.

[76Ros] D E Rosner, H M Chung, and H. H. Feng, J. Chem. Soc., Faraday Trans. I, 1976, 72, p 858

[77Gra] H J Grabke and G Horz, Annu. Rev. Mater. Sci., 1977, 7, p 155

[77Sch] K.schulze and H Jehn, Z. Metallkd., 1977, 68, p 654

[77Kla] R Klauss, 1977, Ph D dissertation Universitat Stuttgart.

[77Ued] Y Ueda, K. Ono and J Moriyama Collected Abstract of the 1977 Autumn Meeting of the Japan Inst Metals, 1977, October, p 202.

[80Fro] E. Fromm and G Horz, Int. Met. Rev., 1980, 25, no. 5-6, p 269

[80Oha] J F O'hanlon "A User's Guide to Vacuum Technology,' 1980, John Wiley & Sons, Inc., New York, p.372

[80Ono] K Ono, Y Ueda, and J Moriyama., Trans. Jpn. Inst. Met., 1980, 21, p.319

[81Eng] C English, "Niobium," Proc. Intl Symp Niobium'81, held in San Francisco, California, 1981, Ed. by H Stuart, p 163

[81Sch1] K. schulze, Obach, D Lupton and F Schreiber, "Niobium," Proc. Intl Symp Niobium'81, held in San Francisco, California, 1981, Ed by H Stuart, p 163

[81Sch2] K. K. Schulze, J. Met., 1981, 33, no 5, p 33

[82Lee] H G Lee and Y K Rao, Metall. Trans. B, 1982, 13, p 411

[82Ono] K. Ono, and J Moriyama, Metall. Trans. B, 1982, 13, p.241

[84Eth] E C Ethridge, P A Curreri, and J Theiss, and G J Abbaschian, Rev. Sci. Instrum., 1984, 55, p 1859

[84Lee] Y K. Rao and H. G Lee, I.S.S. Trans., 1984 4, p 1

[85Asf] R. I. Asfahani, D S Shahapurkar, Y V Murty, J A. Patchett, and G J Abbaschian, J. Met., 1985, 37, no 4, p 22

[85Lee] H. G. Lee and Y K. Rao Ironmaking Steelmaking, 1985, 12, p.221

[85Rao] Y K. Rao, and H G Lee, Ironmaking Steelmaking, 1985, 12, p.209

[85Sch] K Schulze and M Krehl, Nucl. Instrum. Met. in Phys. Res., 1985, A236, p 609

[86Bat] T F Battle, R. D Pehlke, Ironmaking Steelmaking, 1986, 13, p 176

[88Sch] K K Schulze, H. A Jehn, and G Horz, J. Met., 1988 40 no 10, p.25

BIOGRAPHICAL SKETCH

Hyun Gyoon Park was born on July 4, 1954, in Naju, Chon Nam province, Korea. He attended local schools and graduated from Gwang Ju Jeil High School.

In 1973, he matriculated at Seoul National University, graduating with the degree of Bachelor of Science in metallurgical engineering in 1977. He continued his graduate study in materials science and engineering at Korea Advanced Institute of Science and Technology, and received the Master of Science degree in 1979.

After working as a researcher in the area of nuclear materials at Korea Advanced Energy Institute for three and one-half years, he went to the Ohio State University, earning a Master of Science degree in metallurgical engineering in June, 1985.

In the fall of 1985, he entered the Graduate School of University of Florida at Gainesville and has pursued work toward the degree of Doctor of Philosophy in materials science and engineering.

I certify that I have read this study and that in my opinion it conforms to acceptable standards of scholarly presentation and is fully adequate, in scope and quality, as a dissertation for the degree of Doctor of Philosophy

Reza

Reza Abbaschian, Chairman
Professor of Materials Science
and Engineering

I certify that I have read this study and that in my opinion it conforms to acceptable standards of scholarly presentation and is fully adequate, in scope and quality, as a dissertation for the degree of Doctor of Philosophy

Robert T. DeHoff

Robert T. DeHoff
Professor of Materials Science
and Engineering

I certify that I have read this study and that in my opinion it conforms to acceptable standards of scholarly presentation and is fully adequate, in scope and quality, as a dissertation for the degree of Doctor of Philosophy

Paul H. Holloway

Paul H. Holloway
Professor of Materials Science
and Engineering

I certify that I have read this study and that in my opinion it conforms to acceptable standards of scholarly presentation and is fully adequate, in scope and quality, as a dissertation for the degree of Doctor of Philosophy

Brij M. Moudgil

Brij M. Moudgil
Professor of Materials Science
and Engineering

I certify that I have read this study and that in my opinion it conforms to acceptable standards of scholarly presentation and is fully adequate in scope and quality, as a dissertation for the degree of Doctor of Philosophy

Dinesh O Shah
Dinesh O Shah
Professor of Chemical
Engineering

This dissertation was submitted to the Graduate Faculty of the College of Engineering and to the Graduate School and was accepted as partial fulfillment of the requirements for the degree of Doctor of Philosophy

December 1990

Herbert C. Bevis
for Winfred M Phillips
Dean College of Engineering

Madelyn M Lockhart
Dean Graduate School